

# Persistent current and zero-energy Majorana modes in a p-wave disordered superconducting ring

Andrea Nava<sup>1</sup>, Rosa Giuliano<sup>2</sup>, Gabriele Campagnano<sup>3</sup>, and Domenico Giuliano<sup>2</sup>

<sup>1</sup> *Scuola Superiore di Studi Avanzati (SISSA), Via Bonomea 265, I-34136 Trieste, Italy*

<sup>2</sup> *Dipartimento di Fisica, Università della Calabria Arcavacata di Rende I-87036, Cosenza, Italy and I.N.F.N., Gruppo collegato di Cosenza, Arcavacata di Rende I-87036, Cosenza, Italy*

<sup>3</sup> *CNR-SPIN, Monte S. Angelo-Via Cintia, I-80126, Napoli,*

*Italy and Dipartimento di Fisica "E. Pancini", Università di Napoli "Federico II", Monte S. Angelo-Via Cintia, I-80126 Napoli, Italy*

(Dated: July 15, 2018)

We discuss the emergence of zero-energy Majorana modes in a disordered finite-length p-wave one-dimensional superconducting ring, pierced by a magnetic flux  $\Phi$  tuned at an appropriate value  $\Phi = \Phi_*$ . In the absence of fermion parity conservation, we evidence the emergence of the Majorana modes by looking at the discontinuities in the persistent current  $I[\Phi]$  at  $\Phi = \Phi_*$ . By monitoring the discontinuities in  $I[\Phi]$ , we map out the region in parameter space characterized by the emergence of Majorana modes in the disordered ring.

PACS numbers: 73.23.Ra, 74.81.g, 74.45.+c, 73.23.-b

## I. INTRODUCTION

Majorana fermions, particles coinciding with their own antiparticles, were proposed by Majorana in 1937<sup>1</sup>. While, so far, they have never been detected in a particle physics experiment in the last years, after Kitaev's proposal that Majorana fermions may appear as zero-energy real fermionic modes ["Majorana modes" - MMs] localized at the interface between a p-wave one-dimensional superconductor and a normal metal<sup>2</sup>, the search for Majorana fermions in such systems has become one of the most relevant and promising areas in condensed matter physics<sup>3</sup>.

Besides Kitaev's proposal, the emergence of MMs in condensed matter systems has been predicted in a number of systems such as superconductor-topological insulator interfaces<sup>4-7</sup>, in proximity-induced superconducting quantum wires with strong spin-orbit interaction<sup>8-11</sup>, in helical magnets<sup>12</sup>, in ferromagnetic atoms in proximity to superconductors<sup>13,14</sup>. In this context, interesting phases with unconventional properties have been predicted at junctions between topological superconductors, hosting MMs at their endpoints, and interacting one-dimensional electronic systems (Luttinger liquids)<sup>15-17</sup>. In addition, MMs emerging at junctions of one-dimensional interacting quantum wires<sup>18-21</sup>, or of systems formally described as interacting electronic systems, such as quantum Ising spin chains<sup>22-25</sup>, one-dimensional XX-<sup>26</sup>, or XY-<sup>27</sup> models, or pertinently designed Josephson junction networks<sup>28</sup>, have been predicted to give rise to the so-called "Topological Kondo Effect", a remarkable realization of Kondo Effect in which the impurity spin, determined by the MMs, is nonlocal in the wire indices and, thus, cannot be expressed as a functional of local operators<sup>18,19</sup>. Finally, it is worth mentioning that, besides being of remarkable interest for fundamental physics, MMs are also of great interest for quantum computation since, due to their nonabelian statistics<sup>29</sup>, they appear to be among the most natural candidates to work as robust qubits<sup>30</sup>.

The proliferation of theoretical literature about Majorana fermions in condensed matter systems has triggered a number of experimental attempts to probe MMs in pertinently designed devices. The main route followed in the experiments consists in measuring the effects in the transport across junctions between topological superconductors and normal metals possibly due to the presence of localized MMs at the interfaces<sup>31-33</sup>. Unfortunately, despite the excitement following early experimental results, the question of whether what is seen in a transport experiment is actually due to the presence of a MM, or to other possible mechanisms, is still debated, with no ultimate answer so far given, mainly because of the high uncertainty about the possible physical processes taking place in the systems when it is connected to the metallic contacts required for a transport experiment<sup>34,35</sup>. It becomes therefore crucial to engineer systems in which the MMs can be detected in noninvasive experiments, different from a transport measurement. In this direction, an interesting proposal has been put forward in Ref.[36], where it was proposed to realize MMs in a frustrated, finite size topological superconducting quantum interference device (SQUID) at pertinent values of the applied magnetic flux piercing the superconducting ring, as well as in Refs.[37,38], where the Majorana zero mode and the persistent spin current are investigated in mesoscopic d-wave-superconducting loops in the presence of spin-orbit interaction and in mesoscopic s-wave superconducting loops. The advantage of such proposals is twofold: on one hand, it implies the possibility of recovering MMs in a finite system, once the applied flux is properly tuned (differently from what happens, for instance, in the Kitaev model, where, rigorously speaking, "true" zero-energy MMs are in general recovered either in the infinite chain limit, or as a result of a challenging fine-tuning of the system parameters<sup>2</sup>); on the

other hand, it provides an example of MMs realized in a controlled way in a system with tunable control parameters, such as a quasi one-dimensional SQUID ring.

In fact, on the theoretical side, in the last years the study of quasi one-dimensional superconducting rings has been taken advantage of the systematic application of effective field theory approaches<sup>39,40</sup>, which allowed to study nontrivial effects arising in pertinently designed one-dimensional superconducting devices, such as frustration of decoherence<sup>41,42</sup>, correlated hopping of pairs of Cooper pairs<sup>43,44</sup>, etc. On the experimental side, the recent progresses made in the fabrication of nanostructures and, in particular, of superconducting and/or hybrid rings, where superconductivity is induced by proximity effect only in part of the ring<sup>45</sup>, provides an excellent level of control on the design and fabrication of systems which are likely to host MMs, at pertinent values of their parameters.

Yet, notwithstanding the good control one may achieve on the fabrication parameters of the system, the unavoidable presence of disorder can still affect the final behavior of the device. In fact, disorder is in general known to have drastic consequences for the properties of one dimensional normal electronic<sup>46</sup> and superconducting systems<sup>47</sup>. Therefore, it is important to clearly spell out the stability of MMs against disorder. For instance, an open, finite-length Kitaev chain Hamiltonian breaks both spin-rotational and time-reversal invariance. Therefore, it fall into class D of the Altland-Zirnbauer "tenfold way" classification of disordered systems in relation to the symmetries of the corresponding Hamiltonian<sup>47,48</sup>. When the chain is within its topological phase, characterized by the presence of MMs, a weak disorder gives rise to rare small-size nontopological regions, embedded within the topological background. At any interface between topological and nontopological regions, additional MMs arise which, for small disorder, hybridize across the nontopological region into Dirac quasiparticle states that start to fill in the gap. On increasing the disorder strength, the nontopological regions start to proliferate. The corresponding proliferation of MMs and, correspondingly, of subgap states, strongly renormalizes the density of states (DOS) inside the gap, eventually leading to low-energy singularities because of the Griffiths effect in the finite wire<sup>47,49,50</sup>. At strong disorder, the hybridization between MMs at the endpoints of the chain and zero-modes located at the interfaces between topological and nontopological regions eventually washes out the former ones, thus driving the system across a disorder-induced topological phase transition<sup>47,49-56</sup>.

In this paper, we discuss the emergence of MMs at a disordered finite-length p-wave one-dimensional superconducting ring (PSR), pierced by a magnetic flux  $\Phi$  [which, throughout the whole paper, we measure in units of the quantum of flux  $\Phi_0^* = hc/(2e)$ ]. In the absence of disorder, due to the finite size of the system, in general one expects not to find "true" MMs at zero energy, but rather two finite-energy subgap Dirac modes, due to the hybridizations between the MMs through the finite length of the system, into two "putative Majorana fermions" (PMFs), whose energies  $\pm\epsilon_0[\Phi]$  are disposed symmetrically with respect to the Fermi level<sup>2</sup>. Nevertheless, we show that, under quite generic conditions on the PSR parameters, in the absence of disorder it is always possible to tune  $\Phi$  at a value  $\Phi_*$  (that is a function of the parameters of the ring) at which the subgap modes appear exactly at zero energy, due to the level crossing (LC) between the PMF energy levels, thus giving back two true zero-energy MMs.

To probe the PMF LC, we look at the dependence of the persistent current induced in the ring by the applied flux,  $I[\Phi]$ , with respect to  $\Phi$ . In the absence of fermion parity (FP) conservation (which is quite a natural assumption in a quasistatic process), at any PMF LC the PSR relaxes to the minimum energy states, thus triggering a discontinuity in  $I[\Phi]$  at  $\Phi = \Phi_*$ . Therefore, in a clean PSR, discontinuities in  $I[\Phi]$  are uniquely associated to the emergence of zero-energy MMs. The key point of our paper is that this correspondence is preserved in the presence of (a limited amount of) disorder. Specifically, on introducing disorder in the ring and looking at the discontinuities in  $I[\Phi]$  at  $\Phi = \Phi_*$  we identify a region in the parameter space (strength of disorder - chemical potential plane), in which  $I[\Phi]$  is discontinuous at any realization of disorder. We therefore interpret this result as an evidence for the emergence of MMs at the ring even in the presence of disorder. According to this criterion, we map out the corresponding region in the strength of disorder - chemical potential phase plane, which we refer to as "putative topological phase" (PTP). We find that, while, on one hand, the PTP derived within our method strongly resembles the one found for an infinite Kitaev chain by using transfer matrix (TM) approach<sup>55,56</sup>, in our case the actual phase boundary appears broadened, as it must be as a consequence of Griffiths effect for the finite chain near by the phase transition<sup>49,50</sup>. Nevertheless, differently from the TM technique, our approach can be readily implemented as an actual experimental procedure: it is enough to map out the persistent current and to look at possible discontinuities as a function of the applied flux.

We regard our result in the clean limit as a generalization of the derivation of Ref.[36] to a generic p-wave superconducting ring with a weak link. The crucial requirements for our approach to work are the absence of FP conservation and the existence of a LC at  $\Phi = \Phi_*$ , which leads to a  $2\pi$ -periodicity of  $I[\Phi]$ , with a discontinuity at  $\Phi = \Phi_*$ . In this respect, despite the apparent similarity in the discussed device, our approach is fully complementary to the one discussed in Ref.[54]. Indeed, to probe the emergence of subgap PMF levels, in Ref.[54] a nonzero hybridization between the localized MMs is required to take place via the p-wave superconducting region. This assures the persistence of a  $4\pi$ -periodic component of  $I[\Phi]$  even in the absence of FP conservation, which avoids the LC at  $\Phi_*$  just because of the opening of the hybridization gap. Accordingly, the main challenge in probing the PMFs in the presence of disorder just relies on detecting the corresponding survival of the  $4\pi$ -harmonics in the current. Instead, we do assume

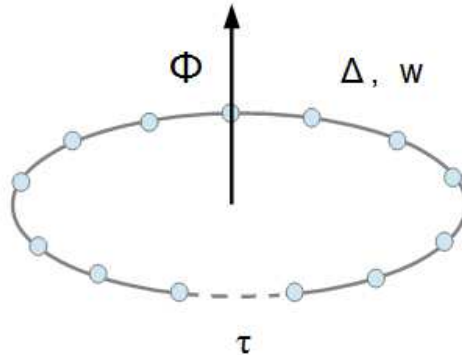


FIG. 1: Sketch of the one-dimensional p-wave superconducting ring pierced by a magnetic flux  $\Phi$  described by  $H_K$  in Eq.(1) plus  $H_\tau[\Phi]$  in Eq.(2).

that there is no hybridization between the MMs via the finite length of the p-wave superconductor. This yields a  $2\pi$ -periodicity of  $I[\Phi]$ , with a discontinuity at  $\Phi = \Phi_*$  that, in our approach, becomes the main fingerprint of the emergence of PMFs, in the clean as well as in the disordered ring.

The paper is organized as follows:

- In Sec. II we present the system Hamiltonian for the PSR in the absence of disorder, review the calculation of the persistent current and discuss the conditions under which subgap PMFs undergo a LC at some value  $\Phi_*$  of the flux  $\Phi$ . Eventually, we discuss the relation between PMF LCs and discontinuities in  $I[\Phi]$ .
- In Sec. III, we perform a detailed analysis of the DOS in the presence of disorder, with particular emphasis onto the subgap PMFs and on their dependence on  $\Phi$ . We show that, provided the system parameters in the "clean" limit are chosen so that there is a PMF LC, the LC survives the presence of disorder so that either there are still PMF states and they cross at a pertinent value of  $\Phi$ , or PMF states are washed out by strong disorder and, accordingly, the zero-energy LC disappears.
- In Sec. IV, we show how the relation between PMF LCs and discontinuities in  $I[\Phi]$  extends to the disordered PSR. Eventually, we use this result to map out the whole PTP in the disorder strength-chemical potential plane.
- In Sec. V, we summarize and comment our results and provide possible further developments of our work.
- In Appendix A, we review the derivation of the eigenvalues and of the eigenfunctions of the open Kitaev chain, with particular emphasis onto subgap states.
- In Appendix B, we review the derivation of the eigenvalues and of the eigenfunctions of the PSR. In particular, we find under which conditions on the system parameters there is a PMF LC at  $\Phi = \Phi_*$  and find an exact formula for  $\Phi_*$  in terms of the system parameters.

## II. MODEL HAMILTONIAN AND SUBGAP STATES

In this section we discuss our system in the absence of disorder. In Fig.1 we provide a sketch of the PSR; it is realized as a p-wave superconducting ring interrupted by a weak normal link and pierced by a magnetic flux  $\Phi$ , which induces a persistent current  $I[\Phi]$  through the system. To formally describe the p-wave superconductor we use Kitaev's one-dimensional lattice model Hamiltonian (KMH)<sup>2</sup>. KMH can be regarded as an effective low-energy description of a quantum wire with a strong spin-orbit coupling and a large enough Zeeman effect, which turns into a one-dimensional p-wave superconductor by proximity to a "standard" s-wave bulk superconductor<sup>8,9</sup>.

The Kitaev lattice Hamiltonian for a one-dimensional p-wave superconductor is given by<sup>2</sup>

$$H_K = -w \sum_{j=1}^{\ell-1} \{c_j^\dagger c_{j+1} + c_{j+1}^\dagger c_j\} - \mu \sum_{j=1}^{\ell} c_j^\dagger c_j + \Delta \sum_{j=1}^{\ell-1} \{c_j c_{j+1} + c_{j+1}^\dagger c_j^\dagger\} . \quad (1)$$

Following the notation of Ref.[2], in Eq.(1) we denote with  $c_j$  ( $c_j^\dagger$ ) ( $j = 1, \dots, \ell$ ) the single-fermion annihilation (creation) operators defined on site- $j$  of the one-dimensional chain, which satisfy the canonical anticommutation relations  $\{c_j, c_{j'}^\dagger\} = \delta_{j,j'}$ , all the other anticommutators being equal to 0. We then denote with  $w$  and  $\Delta$  respectively the normal single-electron hopping amplitude and the p-wave superconducting pairing, and with  $\mu$  the chemical potential. For the sake of simplicity, without any loss of generality, we further simplify  $H_K$  by choosing  $w = \Delta$  (which does not qualitatively affect the spectrum and the eigenfunctions with respect to the general case) and  $\mu \geq 0$  (the complementary situation  $\mu < 0$  can be easily recovered by symmetry). Besides its mathematical simplicity, it is also worth noticing that the Hamiltonian in Eq.(1) with  $w = \Delta$  takes a precise physical meaning, as it can be obtained from the Hamiltonian for an open quantum Ising chain via Jordan-Wigner transformation<sup>57</sup>.

As we review in Appendix A, in its topological phase, a long open Kitaev chain hosts zero-energy MMs localized at the endpoints of the chain<sup>2</sup>. The MMs can then be combined into a zero-energy Dirac mode, which implies a twofold spectral degeneracy of  $H_K$ , with degenerate eigenstates differing from each other by the total FP corresponding to the zero-energy mode being populated, or empty. For a finite-length chain (that is, with  $\ell$  of the same order as the superconducting coherence length of the p-wave superconductor,  $\xi_0$ ), the MMs are hybridized by means of an overlap matrix element that is  $\sim e^{-\frac{\ell}{\xi_0}}$ . In this case, strictly speaking, MMs are not anymore true eigenstates of  $H_K$ . Instead, one may rather speak of two PMFs that hybridize into a finite-energy Dirac mode, with corresponding disappearance of the fermion-parity related degeneracy. As we review in Appendix A, MMs as well as PMFs only emerge provided  $\frac{2w}{\mu} > 1$ . Strictly speaking, one may dub such a phase "topological" only when MMs lie exactly at zero energy. In general, we rather speak of a PTP, with corresponding PMFs hybridized into nonzero energy Dirac modes. Instead, neither MMs, or PMFs, appear in the spectrum for  $\frac{2w}{\mu} < 1$ . To trade the open Kitaev chain for a PSR, we add to  $H_K$  a normal weak link hopping term  $H_\tau$ . Defining  $\tau$  to be the normal hopping amplitude and taking into account that the applied flux  $\Phi$  can be moved onto the weak link hopping term by means of a simple canonical transformation of the fermionic operators,  $H_\tau$  can be presented as<sup>58</sup>

$$H_\tau[\Phi] = -\tau\{e^{\frac{i}{2}\Phi}c_1^\dagger c_\ell + e^{-\frac{i}{2}\Phi}c_\ell^\dagger c_1\} \quad . \quad (2)$$

In the following, we will use the full Hamiltonian  $H[\Phi] = H_K + H_\tau[\Phi]$  to compute the DOS and the persistent current  $I[\Phi]$ . In general, at temperature  $T$ , the persistent current  $I[\Phi; T]$  is obtained from the free energy  $\mathcal{F}[\Phi; T]$  as (see, for instance, Ref.[59] for a review on this approach)

$$I[\Phi; T] = e\partial_\Phi \mathcal{F}[\Phi; T] \quad . \quad (3)$$

Throughout all our paper we will be focusing onto the  $T = 0$ -limit, in which Eq.(3) becomes

$$I[\Phi] = e\partial_\Phi E_{\text{GS}}[\Phi] \quad , \quad (4)$$

with  $E_{\text{GS}}[\Phi]$  being the total groundstate energy of the system. Therefore, in terms of the energies of the quasiparticle excitations of  $H[\Phi]$ ,  $\{\epsilon_n[\Phi]\}$ , one obtains

$$I[\Phi] = e\partial_\Phi E_{\text{GS}}[\Phi] = e\partial_\Phi \sum_{\epsilon_n < 0} \epsilon_n[\Phi] \quad , \quad (5)$$

with the sum taken, as specified, over negative-energy single-quasiparticle states. In a ring made with a conventional s-wave superconductor, as well as in a ring made with a p-wave superconductor in the nontopological phase,  $I[\Phi]$  is typically a periodic function of  $\Phi$  with period  $2\pi$ . Instead, when the p-wave superconductor is within its topological phase, if FP is conserved, the presence of MMs at the endpoints of the superconductor (and, therefore, at the two sides of the weak link) typically makes  $I[\Phi]$  periodic with period equal to  $4\pi$ <sup>60</sup> (note that, for a finite size ring one should carefully spell out whether the  $4\pi$ -periodicity is really due to FP conservation in the presence of MMs, or is a simple effect of the crossover from a superconducting to a mesoscopic ring as  $\ell \leq \xi_0$ <sup>61</sup>). The  $4\pi$ -periodicity simply derives from the fact that FP conservation forbids relaxations between the two levels  $\pm\epsilon_0[\Phi]$ <sup>54</sup>. This leads to the so-called "fractional Josephson effect" (FJE), which has been proposed as an effective way for evidencing the existence of MMs<sup>60</sup>. In fact, in reality it is quite difficult to avoid FP non-conserving relaxation processes in quasistatic (DC) measurements<sup>54,62</sup> and, to overcome such a limitation, proposals of detecting FJE in nonstatic settings have been put forward in measurements of e.g. AC Josephson effect<sup>63,64</sup>, finite-frequency current noise<sup>65</sup>, and Shapiro steps<sup>66</sup>.

In general, in a PSR, one expects a coexistence of a  $2\pi$ - and of a  $4\pi$ -harmonics, due to the existence of two possible "channels" for the MMs to hybridize into a Dirac mode: through the finite-length p-wave superconducting chain, as well as via the weak link. The presence of the two harmonics and the value of their relative weight can be readily understood from our equation for the energy eigenvalues of the PMFs, Eq.(B20) of Appendix B, and from the exact condition for recovering a PMF zero-energy level crossing at pertinent values of  $\Phi$ , Eq.(B25) of appendix B. Indeed,

from Eq.(B20) one expects that  $E_{\text{GS}}[\Phi]$  and, correspondingly,  $I[\Phi]$  are  $4\pi$ -periodic functions of  $\Phi$ , as they only depend on periodic functions of  $\Phi/2$ . As this picture strongly relies upon assuming FP conservation, which is hard to recover in a quasistatic DC current measurement, in Ref.[54] it was noted that, since FP changing processes are expected to take place via relaxation processes that happen just at the PMF LCs, one may just get rid of LCs by pertinently tuning the system parameters. Formally, we rigorously state it in Eq.(B25) of appendix B, where, we prove that PMF LC takes place at  $\Phi = \Phi_*$ , with  $\Phi_*$  satisfying the equation

$$\frac{2w\tau}{\mu^2 - \tau^2} \cos\left(\frac{\Phi_*}{2}\right) = e^{-(\ell-2)\delta_0} \Rightarrow \cos\left(\frac{\Phi_*}{2}\right) = \frac{\mu^2 - \tau^2}{2w\tau} e^{-(\ell-2)\delta_0} \quad , \quad (6)$$

with  $\delta_0$  defined as

$$\delta_0 = 2 \sinh^{-1} \left\{ \sqrt{\frac{\Delta_w^2}{8w\mu}} \right\} \quad . \quad (7)$$

From Eq.(6) we see that a PMF LC happens whenever the contribution to the splitting energy associated to the MM-hybridization through the finite superconducting chain (that is, the term  $\propto e^{-\ell\delta_0}$ ) becomes equal, though opposite in sign, to the contribution associated to MM-hybridization through the weak link (which is  $\propto \tau$ ). Clearly, as the latter contribution is modulated by  $\cos\left(\frac{\Phi}{2}\right)$ , the level crossing can only happen provided one recovers the condition

$$\left| \frac{\mu^2 - \tau^2}{2w\tau} e^{-(\ell-2)\delta_0} \right| \leq 1 \quad , \quad (8)$$

that is, provided that either the chain is long enough (as  $\delta_0 \sim \xi_0^{-1}$ ), or the coupling  $\tau$  is strong enough, or both. Thus, to avoid PMF LC one has to make it impossible to satisfy Eq.(6) at any value of  $\Phi$ . This strategy was actually pursued in Ref.[54], where the regime complementary to ours was recovered by assuming  $\tau/w \ll 1$  and, at the same time, by considering the PSR close to the topological phase transition, at which  $\xi_0 \rightarrow \infty$ , so to make  $\left| \frac{\mu^2 - \tau^2}{2w\tau} e^{-(\ell-2)\delta_0} \right| \gg 1$ . In this case, the hybridization between the MMs through the finite p-wave superconducting region yields a consistent spectral weight for the  $4\pi$ -harmonics, which appears as a modulation of the  $2\pi$ -periodicity in  $I[\Phi]$ , as a result of the competition between the "Kondo-like" hybridization between the PMFs mediated by the weak link<sup>17</sup>, and the "RKKY-like" interaction mediated by the finite chain length. When going across the phase transition, the PMFs disappear, thus determining a full disappearance of the  $4\pi$ -harmonics and a purely  $2\pi$  periodic persistent current.

Throughout our paper we assume that Eq.(8) is satisfied (differently from what is done in Ref.[54]), and that FP is not conserved. As a consequence of Eq.(8), PMF energies  $\pm\epsilon_0[\Phi]$  *vs.*  $\Phi$  show a sequence of LCs as displayed in Fig.2a, where we plot the PMF energies  $\pm\epsilon_0[\Phi]$  *vs.*  $\Phi$  for a PSR with parameters chosen as outlined in the caption (by comparison, in Fig.2b we draw a similar diagram constructed for an s-wave superconducting ring described by the (spinful) Hamiltonian  $H_s = H_{s\text{-wave}} + H_{s\text{-}\tau}$ , with

$$H_{s\text{-wave}} = -w \sum_{\sigma} \sum_{j=1}^{\ell-1} \{c_{j,\sigma}^{\dagger} c_{j+1,\sigma} + c_{j+1,\sigma}^{\dagger} c_{j,\sigma}\} - \mu \sum_{\sigma} \sum_{j=1}^{\ell} c_{j,\sigma}^{\dagger} c_{j,\sigma} + \Delta \sum_{j=1}^{\ell} \{c_{j,\uparrow} c_{j,\downarrow} + c_{j,\downarrow}^{\dagger} c_{j,\uparrow}^{\dagger}\} \quad , \quad (9)$$

and the weak link Hamiltonian given by

$$H_{s\text{-}\tau} = -\tau \sum_{\sigma} \{e^{\frac{i}{2}\Phi} c_{1,\sigma}^{\dagger} c_{\ell,\sigma} + e^{-\frac{i}{2}\Phi} c_{\ell,\sigma}^{\dagger} c_{1,\sigma}\} \quad .) \quad (10)$$

To illustrate the consequences of the absence of FP conservation, in Fig.3, we plot  $I[\Phi]$  *vs.*  $\Phi$  in two PSRs in the PTP, with parameters set as in caption. In both cases, we see the discontinuity in  $I[\Phi]$  at  $\Phi = \Phi_*$ , with  $\Phi_*$  depending on the system parameters as from Eq.(B25).

For comparison, in Fig.4, we plot  $I[\Phi]$  *vs.*  $\Phi$ , for a s-wave superconducting ring and for a PSR not in the PTP: in both cases  $I[\Phi]$  is a continuous function of  $\Phi$ , with no discontinuities within the whole interval  $[-2\pi, 2\pi]$ . As a comment about the discontinuity in  $I[\Phi]$ , it is worth stressing that, while in the plots in Fig.3, we show the exact result obtained from Eq.(5) by summing over all the quasiparticle levels with  $\epsilon_n < 0$ , the discontinuity is clearly determined only by the change in the slope of the PMF energy at the LC. In fact, this is a consequence of the fact that the levels with energy  $|\epsilon_n| > \Delta_w$ , together with their derivatives, are continuous functions of  $\Phi$ , so that they contribute  $I[\Phi]$  by a component that is a smooth function of  $\Phi$ . To highlight this point, in Fig.5a and in Fig.5b, we plot the energy levels *vs.*  $\Phi$  respectively in a PSR in the PTP, and in a PSR not in the PTP. We see that, in the former plot, LCs at the Fermi level only concern the PMF. Instead, in the latter plot, there are no LCs at all, as expected.



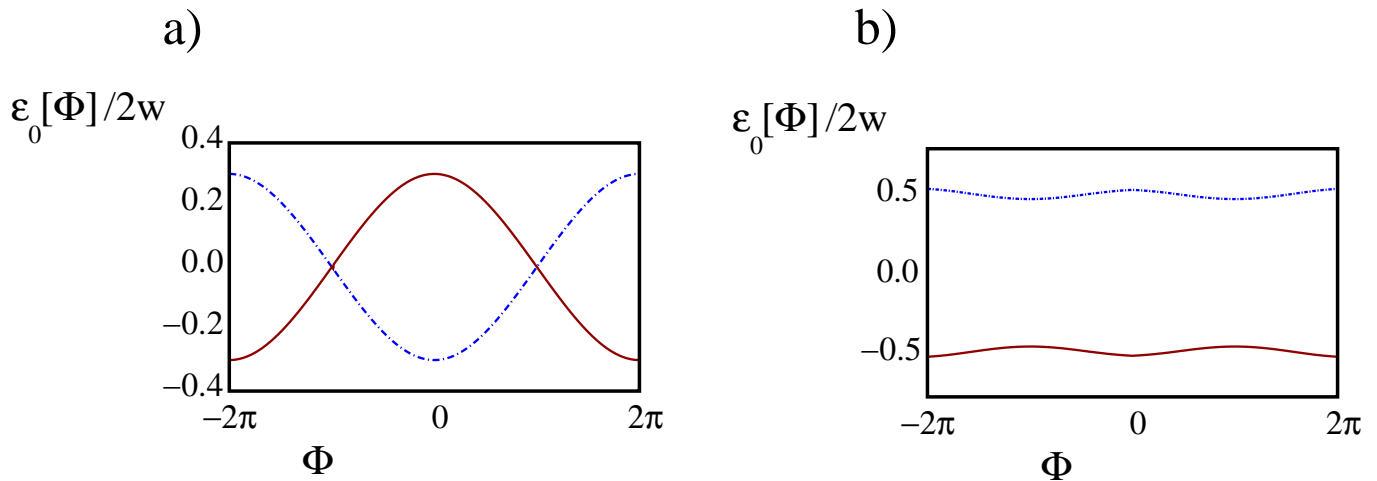


FIG. 2: Subgap energy levels  $\pm\epsilon_0[\Phi]$  as a function of the applied magnetic flux  $\Phi$  for:

**a)** The p-wave superconducting ring with a weak link described by  $H_K$  in Eq.(1) with  $\Delta = w$  plus  $H_\tau$  in Eq.(2) with  $\frac{\mu}{2w} = 0$ ,  $\frac{\tau}{2w} = 0.15$ , and  $\ell = 40$ . At this value of the parameters, one recovers a PMF LC at  $\Phi_* = \pi$ ;

**b)** The s-wave superconducting ring with a weak link described by  $H_{s-wave}$  in Eq.(9) with  $\Delta = w$  plus  $H_{s-\tau}$  in Eq.(10) with  $\frac{\mu}{2w} = 0$ ,  $\frac{\tau}{2w} = 0.15$ , and  $\ell = 40$ . We again see a level modulation with  $\Phi$ , but now the levels emerge nearby the gap edge and keep far from the Fermi level at any value of  $\Phi$ .

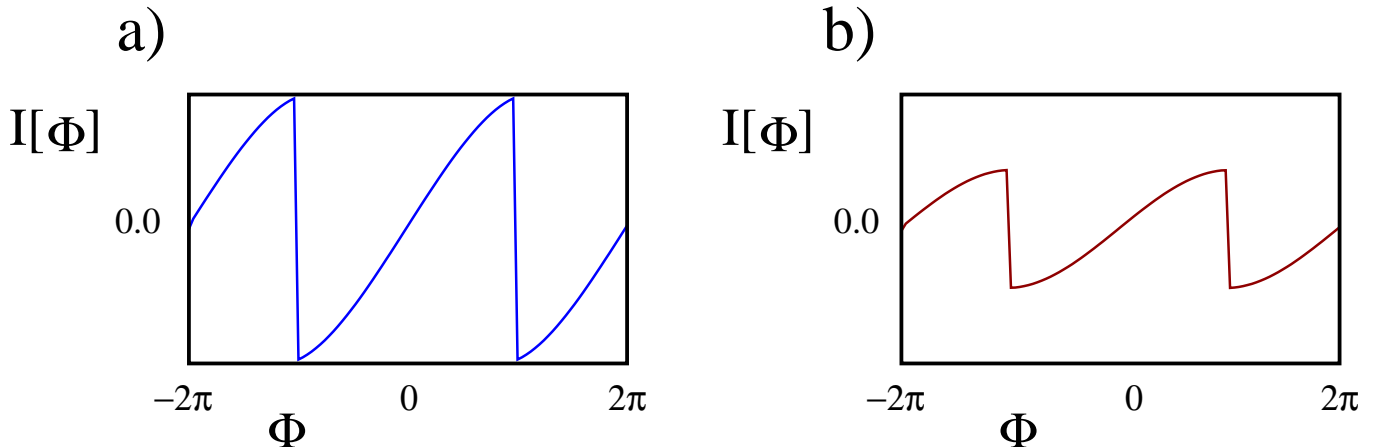


FIG. 3: Persistent current  $I[\Phi]$  (arbitrary units) vs.  $\Phi$  in a p-wave superconducting ring with  $\ell = 40$ ,  $\Delta = w$ , a weak link of strength  $\frac{\tau}{2w} = 0.15$ , and with:

**a)** Chemical potential  $\mu = 0$ ;

**b)** Chemical potential  $\frac{\mu}{2w} = 0.75$ .

The discontinuity of  $I[\Phi]$  at  $\Phi = \Phi_*$  is a readily detectable feature that, under minimal requirements on the system parameters, can be effectively used to mark the existence of a PMF LC by just measuring  $I[\Phi]$  in a static experiment and looking at the specific dependence of the current on the applied flux. As we are going to discuss in the following, this method it can be straightforwardly extended to study to which extent a PMF LC survives in the presence of disorder and, ultimately, to map out the whole PTP.

### III. LOW-ENERGY SUBGAP STATES IN THE PRESENCE OF DISORDER

In the previous section we show that, in the absence of disorder, in a pertinently engineered PSR there always exists a flux  $\Phi = \Phi_*$  at which, due to PMF LC, one recovers the zero-energy MMs  $\gamma_1, \gamma_2$  in Eq.(B29) of Appendix B. In this section, we discuss the robustness of the PMF LC against disorder in the PSR. It is by now established not only that the topological phase survives a moderate amount of disorder in a disordered quantum wire in the presence of a strong spin-orbit coupling and at a large enough Zeeman effect<sup>51–53</sup>, but also that a limited amount of disorder

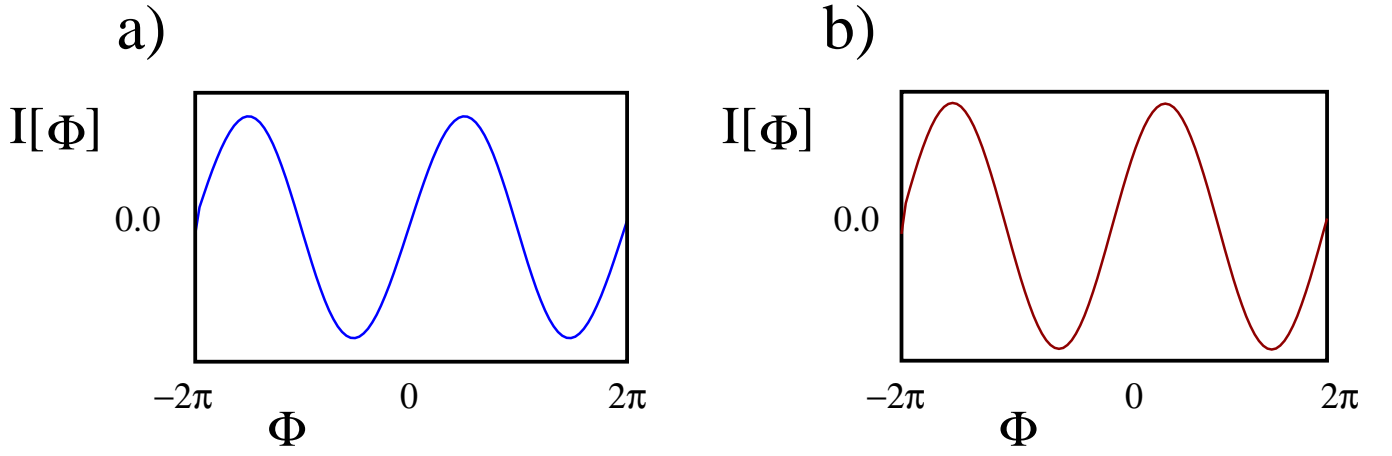


FIG. 4:

**a)** Persistent current  $I[\Phi]$  (arbitrary units) vs.  $\Phi$  in an s-wave superconducting ring with  $\ell = 40$ ,  $\Delta = w$ , a weak link of strength  $\frac{\tau}{2w} = 0.15$ , and  $\mu = 0$  ;  
**b)** Persistent current  $I[\Phi]$  (arbitrary units) vs.  $\Phi$  in a p-wave superconducting ring with  $\ell = 40$ ,  $\Delta = w$ , a weak link of strength  $\frac{\tau}{2w} = 0.15$ , and  $\frac{\mu}{2w} = 1.25$  .

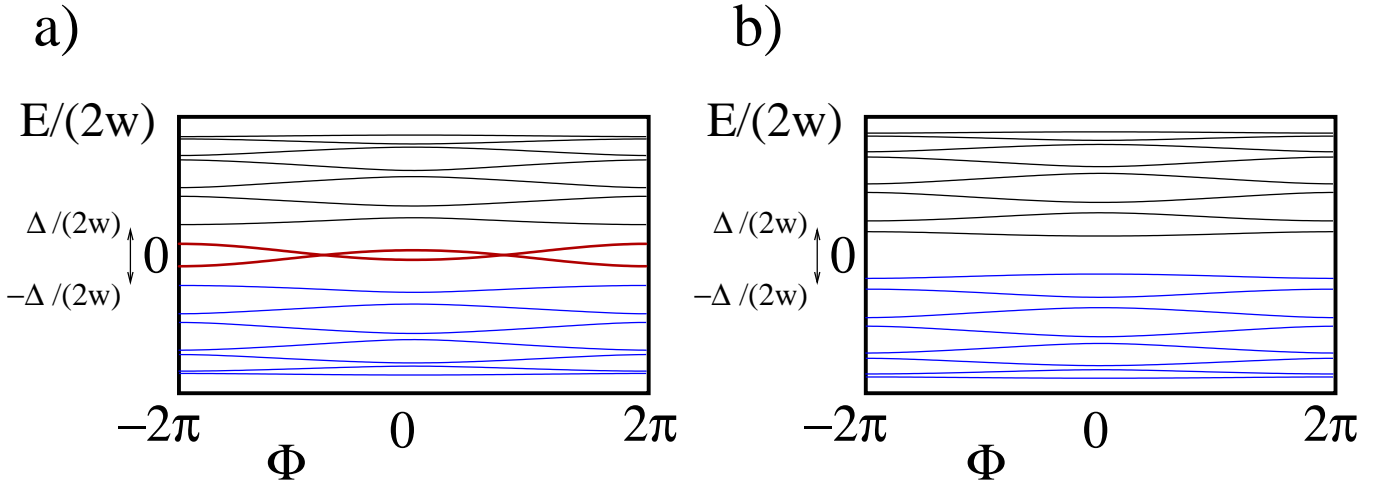


FIG. 5:

**a)** Single-quasiparticle energy levels  $\epsilon_n[\Phi]$  (arbitrary units) vs.  $\Phi$  in a p-wave superconducting ring with  $\ell = 8$ ,  $\Delta = w$ , a weak link of strength  $\frac{\tau}{2w} = 0.25$ , and  $\frac{\mu}{2w} = 0.75$ . The subgap PMFs appearing close to zero-energy are highlighted in red color;  
**b)** Single-quasiparticle energy levels  $\epsilon_n[\Phi]$  (arbitrary units) vs.  $\Phi$  in a p-wave superconducting ring with  $\ell = 8$ ,  $\Delta = w$ , a weak link of strength  $\frac{\tau}{2w} = 0.25$ , and  $\frac{\mu}{2w} = 1.25$ . Consistently with the discussion in the main text, no PMF-levels appear, in this case.

stabilizes the topological phase of an open, infinite Kitaev chain<sup>55,56</sup>. Moreover, it was also stated that moderate disorder does not substantially affect the  $4\pi$ -periodic component of  $I[\Phi]$  in a FP-conserving p-wave superconducting ring with a weak link<sup>54</sup>. Here, instead, we study to what extent the PMF LC in a FP non-conserving PSR is robust against disorder. Specifically, we perform a detailed analysis of the DOS and of the dependence of the energy levels on  $\Phi$ , with particular emphasis onto the PMFs in the presence of disorder. As outlined in the following, we provide numerical evidence that, at a given disorder strength, either subgap PMF energy levels are still present, and they exhibit a LC at a pertinent value of  $\Phi$ , or they are fully washed out by disorder. This leads us to the remarkable conclusion that, as long as PMFs are not washed out by disorder, looking at the discontinuities in  $I[\Phi]$  is still an effective way to probe a PMF LC, exactly as in the absence of disorder.

To model the disorder, we modify the clean system Hamiltonian of Sec. II by adding a random component to the on-site potential, so that, at a fixed disorder realization, the total Hamiltonian  $H = H_K + H_\tau[\Phi]$  is modified as

$$H_K + H_\tau[\Phi] \longrightarrow H_{\{V_j\}}[\Phi] \equiv H_K + H_\tau[\Phi] - \sum_{j=1}^{\ell} V_j c_j^\dagger c_j \quad . \quad (11)$$

The  $\{V_j\}$  are independent random variables described by a probability distribution  $P[\{V_j\}] = \prod_{j=1}^{\ell} p(V_j)$ , with  $p(V)$  being a probability distribution for  $V$  with average  $\bar{V} = \int dV V p(V) = 0$ , and with variance  $\sigma_V^2 = \int dV V^2 p(V)$ , which implies

$$\begin{aligned} \bar{V}_j &= \int \prod_{r=1}^{\ell} dV_r P[\{V_r\}] V_j = 0 \\ \overline{V_i V_j} &= \int \prod_{r=1}^{\ell} dV_r P[\{V_r\}] V_i V_j = \sigma_V^2 \delta_{i,j} \quad , \end{aligned} \quad (12)$$

with  $\overline{O[\{V_j\}]}$  denoting the ensemble average of a generic functional of  $\{V_j\}$  with respect to the probability distribution  $P[\{V_j\}]$ . We use the uniform probability distribution given by

$$p(V) = \begin{cases} \frac{1}{2\sqrt{3}W} & , \text{ for } -\sqrt{3}W \leq V \leq \sqrt{3}W \\ 0 & , \text{ otherwise} \end{cases} \quad , \quad (13)$$

which corresponds to setting  $\sigma_V^2 = W^2$ . We now consider how disorder modifies the single-particle DOS of the ring. In general, for a finite-size system, one expects that the effects of disorder strongly depend on the ratio between the system size  $\ell$  and the disorder-associated mean free path  $l_0$ . In fact, a "weak" disorder, with  $l_0 > \ell$ , is expected to merely quantitatively affect the DOS. In view of the analytical results obtained for an open chain in Ref.[67] within self-consistent Born approximation, later on numerically confirmed in Ref.[50], we expect that a moderate disorder just slightly broadens the subgap peaks corresponding to the PMF energy levels and provides a possible slight renormalization of  $\Phi_*$ , without spoiling the LC. To spell out the effects of increasing disorder strength, we numerically computed the exact single quasiparticle DOS  $\rho(E)$  at increasing  $\sigma_V$  for a PSR in the PTP by using the Hamiltonian in Eq.(11) at fixed  $\{V_j\}$ . Therefore, we ensemble-averaged the result over 300 realization of the disorder. We show the results in Fig.6, where one clearly sees the expected broadening of the subgap peaks, as  $\sigma_V$  increases. At strong disorder ( $l_0 \ll \ell$ ), the energy levels of the system become distributed according symmetry class-D random matrix distribution<sup>46,48,68</sup>. The corresponding level statistics is given by

$$\mathcal{P}[\{\epsilon_j\}] \prod_j d\epsilon_j \propto \prod_{i<j} |\epsilon_i^2 - \epsilon_j^2|^\beta \prod_k [|\epsilon_k|^\alpha e^{-\frac{\epsilon_k^2}{\sigma_V^2}} d\epsilon_k] \quad , \quad (14)$$

with  $\beta = 2$  and  $\alpha = 0$  and the product taken over positive-energy levels only. From Eq.(14) it is possible to extract the single-particle DOS as  $\epsilon \rightarrow 0$ , given by<sup>48</sup>  $\rho(\epsilon) \propto |\epsilon|^\alpha$ . Thus, for symmetry class-D one expects a low-energy uniform DOS, with no evidence of low-lying PMFs. An enlightening discussion of how the disorder washes out PMFs is provided in Ref.[49]: assuming that at zero disorder the system lies within its topological phase, one finds that, for weak disorder, fluctuations in the random potential may open "nontopological islands" within the topological background, of typical size  $\ell_{NT} \ll \ell$ . At each interface between topological and nontopological regions, MMs emerge, which suddenly hybridize into "high-energy Dirac modes", at typical energy scales  $\epsilon_{NT} \sim e^{-\frac{l_0}{\xi_0}}$ , lying below the gap but still higher than the typical energy associated to the "true" PMFs. On one hand, this implies the proliferation of subgap, disorder-induced states. On the other hand, low-energy PMFs are still protected by the very fact that their energies are quite lower than the energies associated to disorder-induced states, and such is the corresponding LC at  $\Phi_*$ . Summarizing, as  $\sigma_V$  increases, one legitimately expects that disorder-induced energy levels fill in the subgap region but also that level repulsion between states with different energy, encoded in  $\mathcal{P}[\{\epsilon_j\}]$  in Eq.(14), acts to "protect" the low-lying PMFs. This is clearly evidenced by the DOS plots we provide in Fig.7, where we show  $\rho(E)$  for a PSR with the same parameters we used to generate Fig.6, but at  $\sigma_V$  such that  $l_0/\ell \sim 0.1$ . We see that, while disorder-induced levels largely fill in the energy gap up to the PMF levels, the regions between the two peaks in Fig.7a are still empty: a signal that the PSR is still within the PTP. Similarly, the persistence of this central peak in Fig.7b due to PMF pile up evidences that the PMF LC at  $\Phi = \Phi_*$  is not spoiled by disorder, even at  $\sigma_V$  as large as  $1.5w$ , consistently with the general expectation about class-D symmetry models<sup>47,69,70</sup>.

In Fig.8 we plot  $\rho(E)$  for a PSR with the same parameters as the ones considered above, but with  $\sigma_V/w = 4.0$ . On comparing Fig.8a to Fig.8b, we see no appreciable differences, that is, we find no detectable differences between the plots at  $\Phi = 0$  and at  $\Phi = \pi$ . In fact, the insensitivity of the DOS to the applied flux can be regarded as a specific



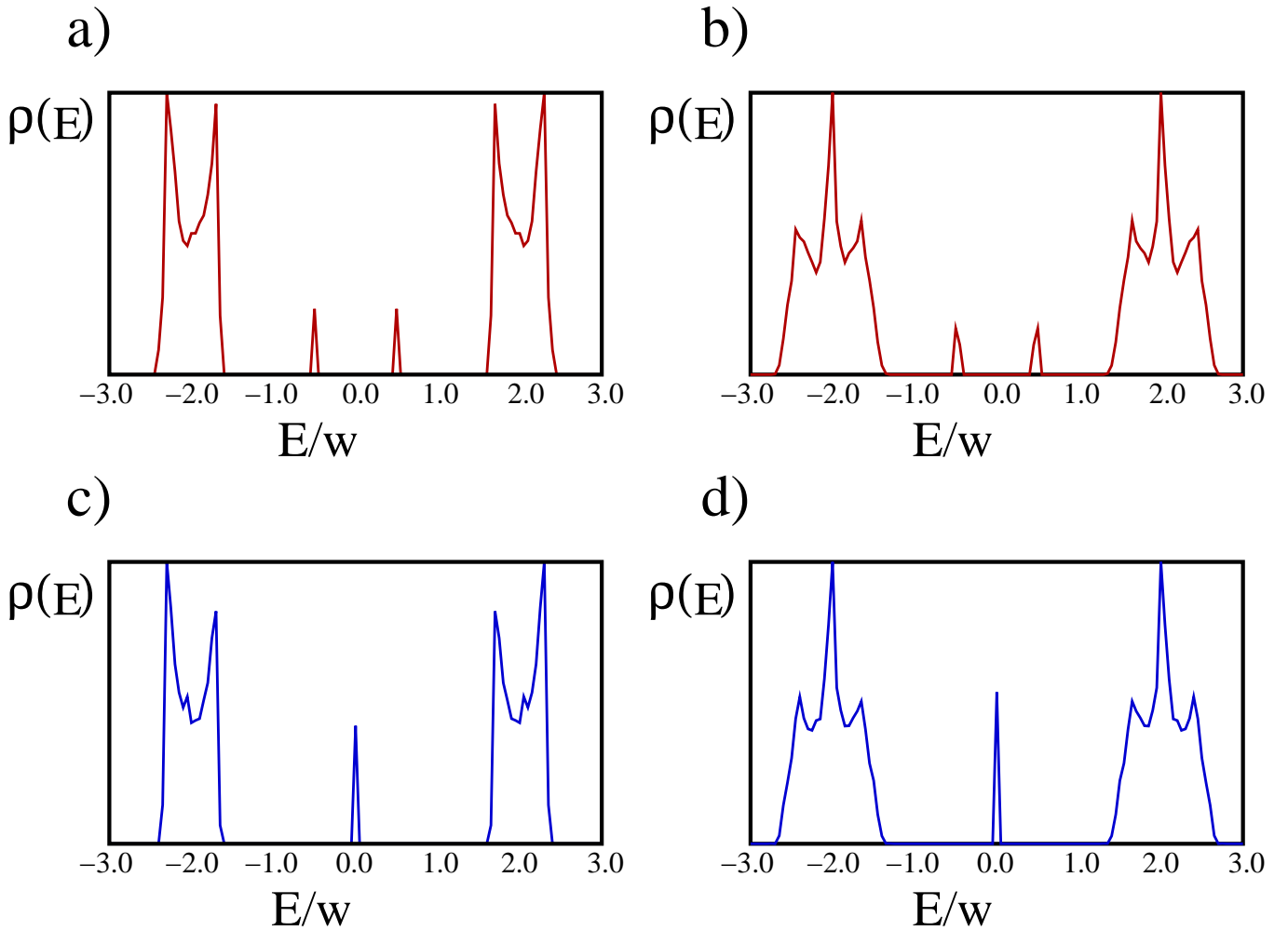


FIG. 6:

Single-quasiparticle DOS  $\rho(E)$  vs.  $E$  for a ring with  $\Delta = w$ ,  $\frac{\mu}{2w} = 0.15$  and  $\frac{\tau}{2w} = 0.25$ , at a given value of the flux  $\Phi$  and of  $\sigma_V$ . The remaining parameters used to generate the plots in the various panels have been set as outlined below:

- a)**  $\Phi = 0$ ,  $\frac{\sigma_V}{w} = 0.05$  (a tiny amount of disorder is added to the clean system for the only purpose of regularizing the divergences at the poles of  $\rho(E)$  corresponding to the single-particle energy eigenvalues);
- b)**  $\Phi = 0$ ,  $\frac{\sigma_V}{w} = 0.3$ . At this value of  $\sigma_V$ , one estimates  $l_0 \sim (2w/\sigma_V)^2 > \ell^{54}$ : as expected from the discussion given in Ref.[50,67], the main effect of increased disorder are the emergence of a finite width for the PMFs and a slight renormalization of the effective superconducting gap;
- c)**  $\Phi = \pi$ ,  $\frac{\sigma_V}{w} = 0.05$ . Same as in panel **a)**, but now the two peaks corresponding to the PMF levels have piled up into a taller peak, evidencing the PMF LC at the Fermi levels;
- d)**  $\Phi = \pi$ ,  $\frac{\sigma_V}{w} = 0.3$ . Same as in panel **b)**, but now the two peaks corresponding to the PMF levels have piled up into a taller peak, evidencing the PMF LC at the Fermi levels.

manifestation of the insensitivity to the boundary conditions (such as the one imposed by the applied flux  $\Phi$  on the single-quasiparticle wavefunction) of the energy levels corresponding to localized states<sup>71,72</sup>. This observation leads us to conclude that all the states filling in the gap at strong disorder are disorder-induced states, while strongly  $\Phi$ -sensitive PMFs have been completely washed out. To further ground our conclusion, in Fig.9a, we plot the first quasiparticle energy levels of the PSR  $\epsilon_n[\Phi]$  vs.  $\Phi$  at  $\sigma_V/w = 2.2$  for a fixed disorder configuration. We clearly see a set of disorder-induced states (drawn in red in the figure) which exhibit a weak dependence on  $\Phi$  and are situated symmetrically with respect to 0 energy, consistently with the survival of particle-hole symmetry against disorder. The states closest to the Fermi level (depicted in blue in the figure) are, instead, to be clearly identified with PMFs. They take a strong dependence on  $\Phi$  and cross with each other at pertinent values of  $\Phi$ . In Fig.9b, we draw a similar plot, but realized for  $\sigma_V/w = 4.2$ . The much larger amount of disorder has determined the full disappearance of PMFs<sup>55</sup>: there are no blue states, but only red impurity states, basically independent of  $\Phi$  (a clear signal of strong localization of these states).

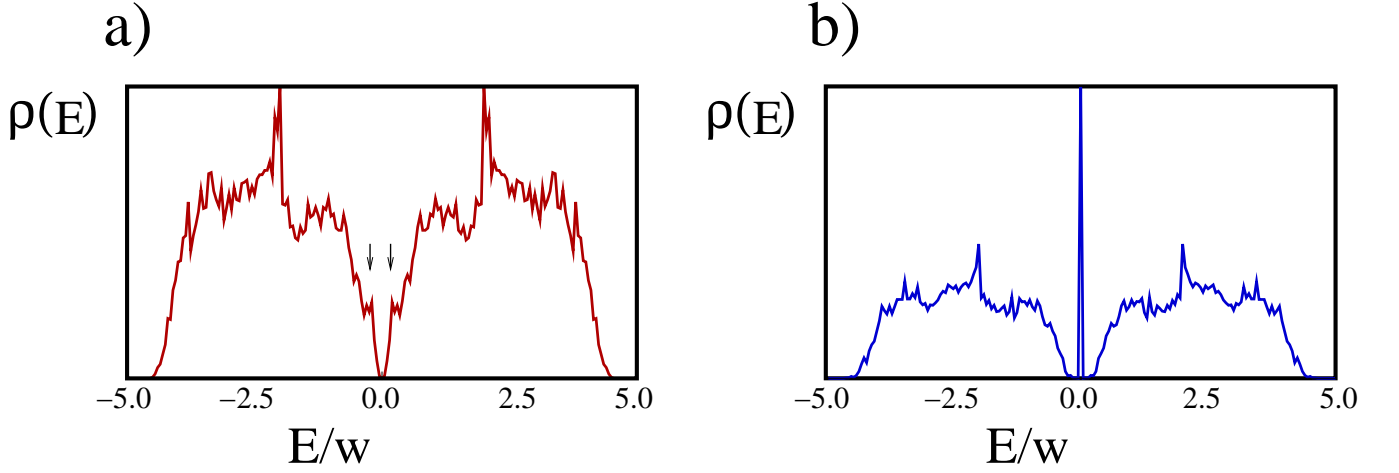


FIG. 7:

Single-quasiparticle DOS  $\rho(E)$  vs.  $E$  for a ring with  $\Delta = w$ ,  $\frac{\mu}{2w} = 0.15$  and  $\frac{\tau}{2w} = 0.25$ , at a given value of the flux  $\Phi$  and of  $\sigma_V$ . The remaining parameters used to generate the plots in the various panels have been set as outlined below :

- a)  $\Phi = 0$ ,  $\frac{\sigma_V}{w} = 1.5$  (the small black arrows highlight the peaks corresponding to the PMF energy levels);
- b)  $\Phi = \pi$ ,  $\frac{\sigma_V}{w} = 1.5$ .

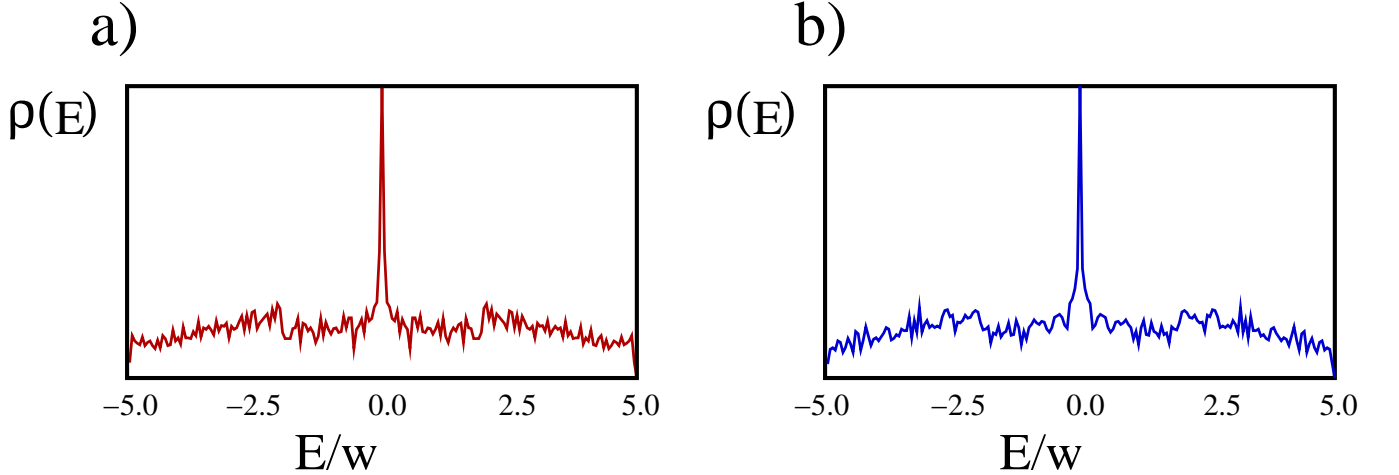


FIG. 8:

Single-quasiparticle DOS  $\rho(E)$  vs.  $E$  for a ring with  $\Delta = w$ ,  $\frac{\mu}{2w} = 0.15$  and  $\frac{\tau}{2w} = 0.25$ , at a given value of the flux  $\Phi$  and of  $\sigma_V$ . The remaining parameters used to generate the plots in the various panels have been set as outlined below:

- a)  $\Phi = 0$ ,  $\frac{\sigma_V}{w} = 4.0$ ;
- b)  $\Phi = \pi$ ,  $\frac{\sigma_V}{w} = 4.0$ .

The peak centered at  $E = 0$  in the plots of Fig.8 corresponds to Griffith's singular behavior in the DOS cutoff at the finite level spacing  $\delta_0 \sim 2\pi w/\ell^{47}$ . In fact, on increasing  $\sigma_V$ , the disorder washes out the PMFs via the Griffiths effect taking place in the finite wire<sup>49,50</sup>. When the nontopological regions start to proliferate, the increasing probability of hybridization between PMFs and zero-modes located at the interfaces between topological and nontopological regions eventually washes out the PMFs themselves, together with the degenerate point at  $\Phi = \Phi_*$ , driving the system outside of the PTP<sup>49,50</sup>.

#### IV. PUTATIVE TOPOLOGICAL PHASE BOUNDARIES AND DISCONTINUITIES IN THE PERSISTENT CURRENT

To discuss the correspondence between PMF LCs and discontinuities in  $I[\Phi]$  in a disordered PSR, we look at the ensemble averaged DOS at fixed  $\sigma_V$  as a function of  $\Phi$ ,  $\rho(E)$ . To numerically construct  $\rho(E)$ , we collect the

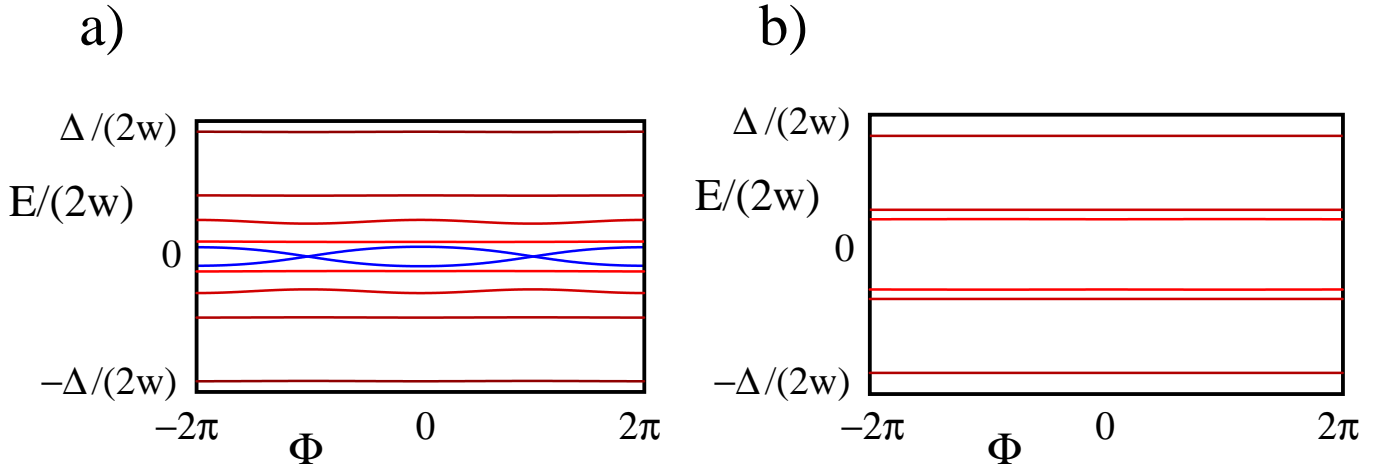


FIG. 9:

a) Sub-gap energy levels  $\epsilon_n[\Phi]$  computed for one realization of the disorder potential in a p-wave superconducting ring with  $\ell = 40$ ,  $\Delta = w$ , a weak link of strength  $\frac{\tau}{2w} = 0.25$ ,  $\frac{\mu}{2w} = 0.75$ , and  $\frac{\sigma_V}{w} = 2.2$ . The subgap PMFs appearing close to zero-energy are highlighted in blue color;

b) Sub-gap energy levels  $\epsilon_n[\Phi]$  computed for one realization of the disorder potential in a p-wave superconducting ring with  $\ell = 40$ ,  $\Delta = w$ , a weak link of strength  $\frac{\tau}{2w} = 0.25$ ,  $\frac{\mu}{2w} = 0.75$ , and  $\frac{\sigma_V}{w} = 4.2$ . No subgap PMFs appear in this case.

eigenvalues generated via an exact Hamiltonian diagonalization procedure into bins defined in the  $E$ - $\Phi$  plane and eventually average over the disorder with  $p(V)$  given in Eq.(13). We thus generate three-dimensional plots of  $\rho(E)$  as a function of both  $E$  and of  $\Phi$  for  $E$  ranging throughout the interval  $[-E_C, E_C]$ , with the half-bandwidth  $E_C = 2w + \mu$  and  $\Phi \in [-2\pi, 2\pi]$ . These are reported in Fig.10 for a PSR in the PTP at limited disorder. In Fig.10, despite the presence of disorder, we clearly see the subgap PMFs, which are characterized by their strong dependence on  $\Phi$  (to be contrasted with the observations that all the other levels displayed in the figure are basically independent of  $\Phi$ ) and, more importantly, that there are evident LCs, evidenced by the sharp peaks - a consequence of the two PMFs density pile-up at those points-. The LCs are not washed out by disorder, which implies that, in a sense that we are going to clarify in the following, there is still a sort of discontinuous behavior of  $I[\Phi]$  at  $\Phi = \Phi_*$ .

By contrast, in Fig.11, we plot  $\rho(E)$  with the same parameters as we chose in Fig.10, but with  $\sigma_V/w = 6.0$ . We see that the spectral weight is largely broadened throughout the interval  $[-E_C, E_C]$ , there is no dependence of the energies on  $\Phi$  and, at the same time, the subgap PMFs have disappeared. This confirms the conclusion we reached in Sec. III, that a strong enough disorder is actually effective in washing out the subgap PMFs.

To map out the PTP, we generalize to a disordered PSR the correspondence between PMF LCs and discontinuities in  $I[\Phi]$ . We first divide the region of interest in the  $\sigma_V - \mu$  planes into square bins and define at the center of each bin a function  $F[\sigma_V, \mu]$  which, at the start, is everywhere equal to 0. Then, at each bin  $(\sigma_{V,i}, \mu_j)$ , we extract a realization  $\{V_j\}$  of the disorder with probability having  $\sigma_V = \sigma_{V,i}$  and exactly diagonalize the Hamiltonian  $H_{\{V\};\mu_j}[\Phi]$  obtained from Eq.(11) by setting  $\mu = \mu_j$ . Then, we use the result to compute the corresponding persistent current,  $I_{\{V\}}[\Phi]$ . Therefore, we check whether  $I_{\{V\}}[\Phi]$  exhibits a discontinuity at some value  $\Phi = \Phi_*$ , or not. If yes, we increment  $F[\sigma_{V,i}, \mu_j]$  by 1, otherwise, we leave it unchanged. Specifically, to identify  $\Phi_*$  we discretize the interval of values of  $\Phi$  and, starting from  $\Phi = 0$ , at each step we increment  $\Phi$  by  $\delta\Phi$ , with  $0 < \delta\Phi \ll 2\pi$ . Setting  $\Phi_r = r\delta\Phi$ , we look at the sign of the product  $I[\Phi_r]I[\Phi_{r+1}]$ . As soon as  $I[\Phi_r]I[\Phi_{r+1}] < 0$ , we tentatively identify  $\Phi_*$  with the middle point of the interval  $[\Phi_r, \Phi_{r+1}]$ . We then numerically estimate the slope of  $I[\Phi]$  at  $\Phi_*$  as  $(I[\Phi_{r+1}] - I[\Phi_r])/\delta\Phi$  and at the left-hand side of  $\Phi_*$  as  $(I[\Phi_r] - I[\Phi_{r-1}])/\delta\Phi$ , concluding that  $\Phi_*$  corresponds to a discontinuity point if the two slopes differ from each other by a factor  $\geq 1.5$ . After summing, at each bin, over  $\mathcal{N} = 300$  random realizations of the disorder, we define  $f[\sigma_{V,i}, \mu_j] = F[\sigma_{V,i}, \mu_j]/\mathcal{N}$ , so that  $0 \leq f[\sigma_{V,i}, \mu_j] \leq 1, \forall i, j$ . As a final result, we draw the diagram in Fig.12, where we show a color-scale plot of  $f[\sigma_V, \mu]$  computed for a ring with  $\ell = 60$ ,  $w = \Delta$ , and  $\tau/(2w) = 0.25$ . In detail, we constructed the plot by increasing both  $\sigma_V/w$  and  $\mu/w$  by step of 0.05 and by accordingly defining the bins in the  $\sigma_V - \mu$ -plane. The region marked in full red corresponds to  $f = 1$ , that is, to a current which is singular at some  $\Phi_*$  for any realization of the disorder. Conversely, the white portion of the graph corresponds to  $f = 0$ , that is, to a current that is a continuous function of  $\Phi$  for any realization of the disorder (see Fig.12 for a graphic summary of the color code). Clearly, points in the red region are characterized by PMFs that undergo a LC at  $\Phi = \Phi_*$ , that is, we may identify the red region with the PTP in the presence of disorder. By converse, points in the white region are characterized by the absence of PMFs. The shaded area, where the color

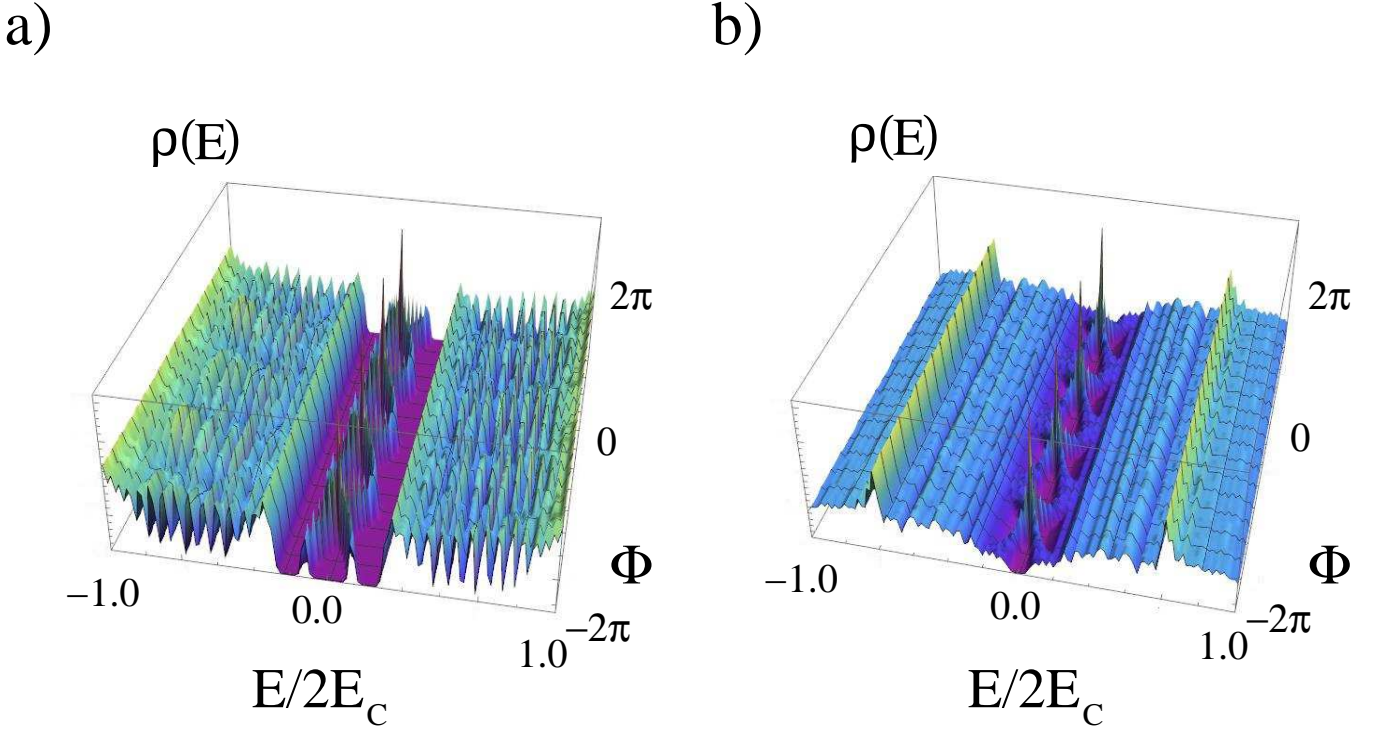


FIG. 10:

**a)** DOS  $\rho(E)$  for a disordered ring described by the Hamiltonian in Eq.(11) with  $\Delta = w$ ,  $\frac{\mu}{2w} = 1.2$ ,  $\frac{\tau}{2w} = 0.25$ ,  $\ell = 40$ , obtained by ensemble-averaging over 100 realization of the disorder with  $\frac{\sigma V}{w} = 0.2$ . The subgap PMFs close to the Fermi level are clearly displayed;

**b)** DOS  $\rho(E)$  for a disordered ring described by the Hamiltonian in Eq.(11) with  $\Delta = w$ ,  $\frac{\mu}{2w} = 1.2$ ,  $\frac{\tau}{2w} = 0.25$ ,  $\ell = 40$ , obtained by ensemble-averaging over 100 realization of the disorder with  $\frac{\sigma V}{w} = 0.8$ . The subgap PMFs are less resolved, but there are clear peaks at the level crossings, due to the pile-up of the DOS of the two PMFs. These peaks survive the transfer of spectral weight from the PMFs to disorder-induced Griffiths states, which evidences that the PSR still lies within the PTP.

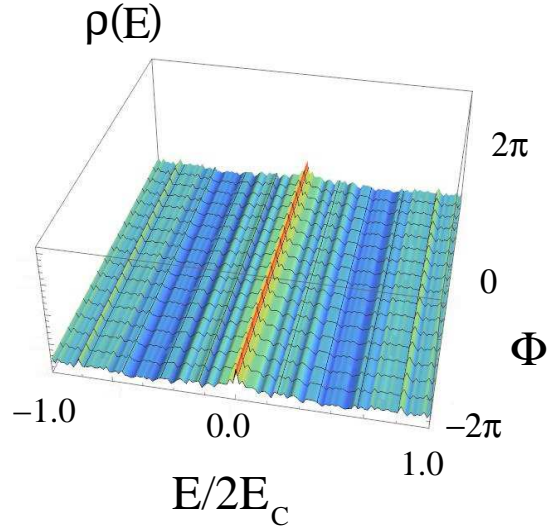


FIG. 11:

DOS  $\rho(E)$  for a disordered ring described by the Hamiltonian in Eq.(11) with  $\Delta = w$ ,  $\frac{\mu}{2w} = 1.2$ ,  $\frac{\tau}{2w} = 0.25$ ,  $\ell = 40$ , obtained by ensemble-averaging over 100 realization of the disorder with  $\frac{\sigma V}{w} = 6.0$ . The spectral density is broadened throughout the interval  $[-E_C, E_C]$ , there is a negligible dependence on  $\Phi$ , and the subgap PMFs have disappeared.

varies from red to white, defines the transition region at which the PTP disappears and the PMFs are washed out of the spectrum. By analogy, one would expect a sharp transition line, such as the one separating the topological from the nontopological phases of the infinite Kitaev chain, drawn in Refs.[55,56] by using transfer matrix method. Nevertheless, we obtain a broad transition region, rather than a sharp phase boundary, because, for each disorder realization we exactly diagonalize a well-defined Hamiltonian, which either presents PMFs with a finite- $\Phi$  LC, or not. Near the phase transition, when averaging over  $\mathcal{N}$  different realization of the disorder, there can be a nonzero probability that some realizations wash out PMFs at values of the system parameters where PMFs are present in the large majority of cases or, conversely, that PMFs appear at points in parameter space where they are absent in the large majority of cases. To be more precise, when the system lies within the PTP, strong fluctuations in the mean value of the impurity potential on a single realization of disorder may drive it outside of the PTP, and vice versa. As a result, close to the point of disappearance of the PTP, we expect that, on ensemble averaging over disorder, the percentage of single disorder realizations respectively leading to a discontinuous, or to a continuous, current will be both different from zero (incidentally, we note that this is quite a common feature of finite system undergoing a Griffith phase transition<sup>50</sup>). Instead, far from the transition there is no ambiguity in that either  $I[\Phi]$  is discontinuous, or continuous for any realization of disorder, just as we can see from the plot of  $f[\sigma_V, \mu]$  in Fig.12. Eventually, to map out the (broad) phase boundary of the PTP in the disorder strength-chemical potential plane, we start from within the PTP at zero disorder strength. Then, we move along the horizontal axis at fixed  $\mu$  by probing the existence of the discontinuity in  $I[\Phi]$  at increasing  $\sigma_V$ : for  $0 \leq \mu/w < 2$  and for  $\sigma_V = 0$ , we typically obtain  $f[0, \mu] = 1$ . Consistently with the above discussion, at some  $\mu$ -dependent "lower critical" value of  $\sigma_V$ ,  $\sigma_{\mu;l}$ , we start to obtain  $f[\sigma_{V;l}, \mu] < 1$ . This signals the start of the transition region when going across which the PTP disappears. On further increasing  $\sigma_V$ , one typically reaches an "upper critical" value,  $\sigma_{\mu;u}$ , such that  $f[\sigma_V; \mu] = 0$  for  $\sigma_V > \sigma_{\mu;u}$ . Therefore,  $\sigma_{\mu;l}$  and  $\sigma_{\mu;r}$  determine the transition region at a given  $\mu$  as the set of points  $(\sigma_V, \mu)$  such that  $\sigma_{\mu;l} < \sigma_V < \sigma_{\mu;u}$ . Repeating the procedure along constant- $\mu$  lines, we mapped out the full color scale plot of  $f[\sigma_V, \mu]$  in Fig.12.

Besides the broadening related to the Griffith mechanism, Fig.12 shows a remarkable analogy with the phase diagram for a long Kitaev chain with open boundary conditions reported in Fig.1 of Ref.[55]. In particular, the two diagrams share the remarkable feature of a reentrant topological phase at not-too-large values of  $\sigma_V$ , that is, a small amount of disorder appears to favor, rather than suppressing, the topological phase. In our specific finite-size ring, we interpret the reentrant phase as an effect of the disorder-induced renormalization of the chemical potential which, at nonzero  $\sigma_V$ , pushes the phase transition to values of  $\mu$  higher than the zero-disorder critical value  $\mu_c = 2w$ , or lower than  $\mu_c = -2w$  (a detailed discussion of this effect, both using the reduced effective low-energy Hamiltonian for the ring and in general, as a consequence of turning on a weak disorder, is provided in Refs.[53,54]). As discussed above, the finite width of the transition region has to be regarded as a consequence of the Griffiths mechanism in a finite system<sup>50</sup>: in the  $\ell \rightarrow \infty$  limit and after averaging over a large number of realizations of disorder, the transition region is nevertheless expected to shrink to a sharp phase boundary, coinciding with the solid black line of Fig.1 of Ref.[55].

Fig.12 summarizes the key results of this paper: on one hand, it can be regarded as a theoretical derivation of the region, in the  $\sigma_V - \mu$  plane, in which it is possible to make two zero-energy MMs emerge at the quantum ring by pertinently acting on the applied flux. On the other hand, the way we derived it suggests a practical tool to map it out in an actual experiment: to check whether, at a given values of the system parameters, zero-energy MMs are recovered at a disordered PSR, it is enough to probe the dependence of  $I[\Phi]$  on  $\Phi$  and to check whether, at some flux  $\Phi = \Phi_*$  (with  $\Phi_*$  typically being  $\sim \pi$  for a not-too-short chain),  $I[\Phi]$  shows a discontinuous behavior, with a finite jump when going across  $\Phi_*$ . A key point of our proposed technique is that  $I[\Phi]$  can in principle be probed by means of a noninvasive magnetometer, without need for contacting the system as one has to do in a transport experiment attempting to probe MMs<sup>31</sup>; this potentially should avoid problems related to the introduction of sources of noise in the system. Moreover, we recall that the techniques so far proposed to map out the phase diagram of a disordered Kitaev-like chain, mostly rely on looking at the eigenvalues of the transfer matrix of the whole chain<sup>55,56</sup>: an approach rigorous and effective from the mathematical point of view, but lacking the possibility of a direct experimental implementation. At variance, as stated above, in order for our approach to work in practice, one simply needs to perform a noninvasive magnetic probe, thus providing a direct means to measure the emergence of MMs in the ring at an appropriate value of the applied flux.

From the physical point of view, our numerical findings prove that zero energy MMs emerging in a quantum ring at  $\Phi = \Phi_*$  are quite robust against disorder. It would be extremely interesting to perform a rigorous analytical investigation of the features of the PMFs and of the stability of the MMs at  $\Phi = \Phi_*$ : this topic lies nevertheless beyond the scope of this work and we plan to investigate it in a forthcoming publication.

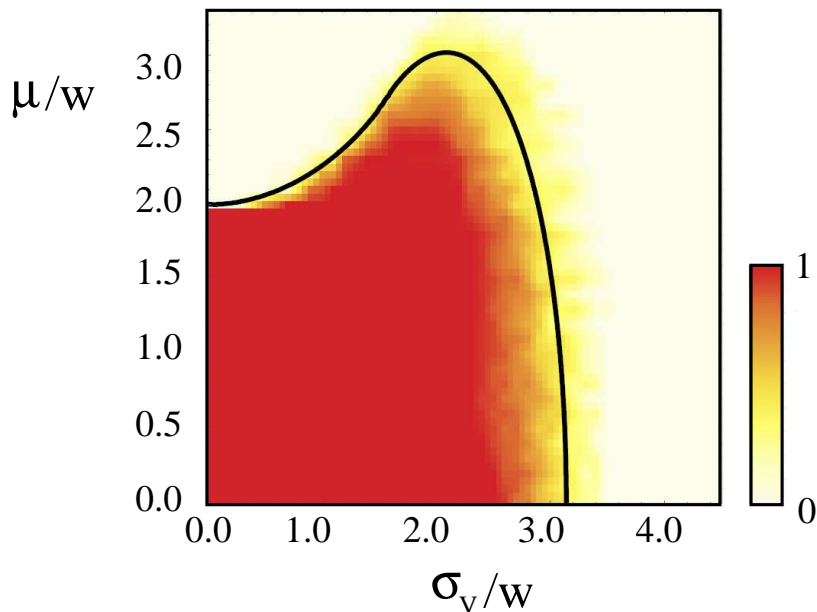


FIG. 12: Color-scale plot of  $f[\sigma_V, \mu]$  in the  $\sigma_V - \mu$  plane. The color code is summarized at the right-hand side of the plot. The shaded region, where the color varies from red to white, defines the transition region at which the PTP disappears and the PMFs are washed out of the spectrum. The red line is a sketch of the variation of the center of mass of the transition region as a function of  $\mu$ : in the  $\ell \rightarrow \infty$  limit and after averaging over a large number of realizations of disorder, it is expected to coincide with the solid black line of Fig.1 of Ref.[55].

## V. CONCLUSIONS AND FURTHER PERSPECTIVES

In this paper, we discuss the emergence and a way for probing MMs at a disordered finite-length p-wave one-dimensional superconducting ring, pierced by a magnetic flux  $\Phi$ , in the absence of FP conservation. We prove that, at a moderate amount of disorder, it is still possible to tune  $\Phi$  at a value  $\Phi_*$  at which the subgap modes appear exactly at zero energy, due to the level crossing between the subgap energy levels. At  $\Phi = \Phi_*$ , the MMs are recovered as pertinent linear combinations of the subgap mode operators. To probe the level crossing, we propose to look for discontinuities in the persistent current  $I[\Phi]$  at  $\Phi = \Phi_* \sim \pi$ . On pertinently employing our technique, we map out the whole region, in the disorder strength-chemical potential plane, characterized by zero-energy subgap LCs. At this point, we expect it to be possible to realize in a controlled and tunable way MMs which, in principle, provide a crucial and effective resource for designing efficient quantum computation protocols.

In the presence of disorder, our results mostly rely on a numerical analysis: while it would be extremely interesting to perform a rigorous analytical investigation of the features of the PMFs and of the stability of the MMs at  $\Phi = \Phi_*$ , this is outside the scope of this work and we plan to investigate it in a forthcoming publication.

G. Campagnano acknowledges financial support from MIUR-FIRB 2012 project HybridNanoDev (Grant No. RBFR1236VV). We acknowledge insightful discussions with A. De Martino, L. Lepori, P. Lucignano, A. Romito, and A. Tagliacozzo.

### Appendix A: Excitation spectrum of the open Kitaev chain with $w = \Delta$

In this appendix we review the derivation of the excitation spectrum of the Kitaev Hamiltonian in Eq.(1) defined on an open chain with  $\ell$  sites. Technically, we diagonalize  $H[\Phi]$  at  $\tau = 0$ , that is,  $H_K$ , with open boundary conditions on the single-mode wavefunction. A generic eigenmode, for  $\Delta = w$ , of  $H_K$  with energy  $E$  takes the form

$$\Gamma_E = \sum_{j=1}^{\ell} \{ [u_j]^* c_j + [v_j]^* c_j^\dagger \} \quad , \quad (\text{A1})$$



with the wavefunctions  $u_j, v_j$  solving the appropriate Bogoliubov-de Gennes (BdG) equations obtained from the canonical commutation relation  $[\Gamma_E, H_K] = E\Gamma_E$ . These are given by

$$\begin{aligned} Eu_j &= -w\{u_{j+1} + u_{j-1}\} - \mu u_j + w\{v_{j+1} - v_{j-1}\} \\ Ev_j &= -w\{u_{j+1} - u_{j-1}\} + w\{v_{j+1} + v_{j-1}\} + \mu v_j \quad , \end{aligned} \quad (\text{A2})$$

for  $1 < j < \ell$ . At the endpoints ( $j = 1, \ell$ ), the equations take the form

$$\begin{aligned} Eu_1 &= -wu_2 + wv_2 - \mu u_1 \\ Ev_1 &= -wu_2 + wv_2 + \mu v_1 \quad , \end{aligned} \quad (\text{A3})$$

and

$$\begin{aligned} Eu_\ell &= -wu_{\ell-1} - wv_{\ell-1} - \mu u_\ell \\ Ev_\ell &= wu_{\ell-1} + wv_{\ell-1} + \mu v_\ell \quad . \end{aligned} \quad (\text{A4})$$

Requiring that Eqs.(A2) are satisfied, the solution for  $1 < j < \ell$  takes the form

$$\begin{bmatrix} u_j \\ v_j \end{bmatrix} = e^{ikj} \begin{bmatrix} u_k \\ v_k \end{bmatrix} \quad . \quad (\text{A5})$$

Imposing the wavefunctions in Eqs.(A5) to be a solution of Eqs.(A2), one gets the system of equations in momentum space, given by

$$\begin{aligned} Eu_k &= -[2w \cos(k) + \mu]u_k + 2iw \sin(k)v_k \\ Ev_k &= -2iw \sin(k)u_k + [2w \cos(k) + \mu]v_k \quad , \end{aligned} \quad (\text{A6})$$

supplemented with the boundary conditions

$$u_0 + v_0 = u_{\ell+1} - v_{\ell+1} = 0 \quad . \quad (\text{A7})$$

From Eqs.(A6), we obtain the dispersion relation (assuming  $\mu > 0$ )

$$E = \pm \sqrt{(2w - \mu)^2 + 8w\mu \cos^2\left(\frac{k}{2}\right)} \quad . \quad (\text{A8})$$

Having defined the actual gap  $\Delta_w$  as  $\Delta_w = |2w - \mu|$ , Eq.(A8) can be inverted, yielding the momentum of an excitation with energy  $E$  as

$$\cos\left(\frac{k}{2}\right) = \pm \sqrt{\frac{E^2 - \Delta_w^2}{8w\mu}} \quad . \quad (\text{A9})$$

Solutions with energy  $|E| > \Delta_w$  correspond to real value of  $k$ . These can be readily written in a compact form, once one defines  $\Psi$  so that

$$\begin{aligned} \cos(\Psi) &= -\frac{2w \cos(k) + \mu}{E} \\ \sin(\Psi) &= \frac{2w \sin(k)}{E} \quad . \end{aligned} \quad (\text{A10})$$

Imposing the boundary conditions in Eq.(A7), one eventually obtains the positive-energy solutions

$$\begin{bmatrix} u_j \\ v_j \end{bmatrix}_+ = \sqrt{\frac{2}{\ell}} \begin{bmatrix} \cos\left(\frac{\Psi}{2}\right) \sin\left(kj + \frac{\Psi}{2}\right) \\ -\sin\left(\frac{\Psi}{2}\right) \cos\left(kj + \frac{\Psi}{2}\right) \end{bmatrix} \quad , \quad (\text{A11})$$

while the corresponding negative-energy solutions are recovered by acting with  $\tau^x$  on the solution in Eq.(A11), that is

$$\begin{bmatrix} u_j \\ v_j \end{bmatrix}_- = \tau^x \begin{bmatrix} u_j \\ v_j \end{bmatrix}_+ = \sqrt{\frac{2}{\ell}} \begin{bmatrix} -\sin\left(\frac{\Psi}{2}\right) \cos\left(kj + \frac{\Psi}{2}\right) \\ \cos\left(\frac{\Psi}{2}\right) \sin\left(kj + \frac{\Psi}{2}\right) \end{bmatrix} \quad . \quad (\text{A12})$$

The secular equation for the allowed values of  $k$  is determined by the boundary condition at  $j = \ell + 1$ . It is given by

$$\sin[k(\ell + 1) + \Psi] = 0 \quad . \quad (\text{A13})$$

Sub-gap PFs are instead recovered for complex values of  $k$ , which are fixed by the condition

$$\cos\left(\frac{k}{2}\right) = \pm i \sqrt{\frac{\Delta_w^2 - E^2}{8w\mu}} \quad . \quad (\text{A14})$$

To solve Eq.(A14), we now define the momentum for particle-like excitations as  $k_p = \pi - i\delta$  and for hole-like excitations as  $k_h = \pi + i\delta$ , with

$$\delta = 2 \sinh^{-1} \left\{ \sqrt{\frac{\Delta_w^2 - E^2}{8w\mu}} \right\} \quad . \quad (\text{A15})$$

As a result, the most general sub-gap eigenfunction with energy  $E > 0$  is given by

$$\begin{bmatrix} u_j \\ v_j \end{bmatrix} = c (-1)^j \begin{bmatrix} \cosh\left(\frac{\xi}{2}\right) \{\alpha e^{j\delta} + \beta e^{-j\delta}\} \\ \sinh\left(\frac{\xi}{2}\right) \{\alpha e^{j\delta} - \beta e^{-j\delta}\} \end{bmatrix} \quad , \quad (\text{A16})$$

with  $\xi$  defined through the equations

$$\begin{aligned} \cosh(\xi) &= \frac{2w \cosh(\delta) - \mu}{E} \\ \sinh(\xi) &= \frac{2w \sinh(\delta)}{E} \quad , \end{aligned} \quad (\text{A17})$$

and the coefficients  $\alpha$  and  $\beta$  determined by the boundary conditions in Eqs.(A7). Clearly, a state with energy  $E > 0$  comes together with the particle-hole conjugated one, with energy  $-E^2$ . In imposing the boundary conditions in Eqs.(A7), one finds that  $\alpha e^{\frac{\xi}{2}} + \beta e^{-\frac{\xi}{2}} = 0$  and, more importantly, that the allowed value of  $E$  must satisfy the condition

$$\sinh[\xi - (\ell + 1)\delta] = 0 \Rightarrow \xi(E) = (\ell + 1)\delta(E) \quad . \quad (\text{A18})$$

Eq.(A18) is a transcendent equation, whose solution can in general only be derived numerically. Yet, a simple approximate formula for the energy can be derived in the long chain limit, where one may assume that the energy is small enough to enable one to neglect the dependence of  $\delta$  on  $E$  and, therefore, to make the approximation

$$\delta(E) \approx \delta_0 = 2 \sinh^{-1} \left\{ \sqrt{\frac{\Delta_w^2}{8w\mu}} \right\} \quad . \quad (\text{A19})$$

Thanks to Eq.(A19), one therefore obtains

$$E \sim \{2we^\delta - \mu\}e^{-\xi} \approx \{2we^{\delta_0} - \mu\}e^{-(\ell+1)\delta_0} \quad . \quad (\text{A20})$$

In general, even without knowing the explicit solution, one can identify the boundary of the phase characterized by the low-lying modes by noting that, in order for Eq.(A18) to be satisfied,  $\xi(E)$  must be real, which implies that  $e^{-\xi(E)} > 0$ . Therefore, one notes that

$$e^{-\xi(E)} = \frac{2we^{-\delta(E)} - \mu}{E} \quad , \quad (\text{A21})$$

which implies that  $\xi(E)$  is real if, and only if,

$$\frac{2w}{\mu} > e^{\delta(E)} = \frac{\sqrt{(2w + \mu)^2 - E^2} + \sqrt{(2w - \mu)^2 - E^2}}{\sqrt{(2w + \mu)^2 - E^2} - \sqrt{(2w - \mu)^2 - E^2}} \geq 1 \quad . \quad (\text{A22})$$

Therefore, the phase characterized by the presence of low-lying PMFs is defined by the condition  $\frac{2w}{\mu} > 1^2$ , even in the case of a finite-length chain.

## Appendix B: Excitation spectrum of the closed ring

In this appendix, we derive the energy eigenvalues and the corresponding eigenmodes of  $H[\Phi]$ . Proceeding as for the open chain, for  $1 < j < \ell$ , the BdG equation take the same form as in Eq.(A2). At  $j = 1$ , one gets

$$\begin{aligned} Eu_1 &= -wu_2 - \tau e^{-\frac{i}{2}\Phi} u_\ell - \mu u_1 + wv_2 \\ Ev_1 &= -wu_2 + wv_2 + \tau e^{\frac{i}{2}\Phi} v_\ell + \mu v_1 \quad , \end{aligned} \quad (\text{B1})$$

while at  $j = \ell$ , one obtains

$$\begin{aligned} Eu_\ell &= -wu_{\ell-1} - \tau e^{\frac{i}{2}\Phi} u_1 - \mu u_\ell - wv_{\ell-1} \\ Ev_\ell &= wu_{\ell-1} + wv_{\ell-1} + \tau e^{-\frac{i}{2}\Phi} v_1 + \mu v_\ell \quad . \end{aligned} \quad (\text{B2})$$

In order for the conditions in Eqs.(B1,B2) to be satisfied, one has to modify the ansatz in Eq.(A5). For the sake of clarity, in the following we shall use  $\bar{u}_1, \bar{v}_1$  and  $\bar{u}_\ell, \bar{v}_\ell$  to respectively denote the wavefunctions at  $j = 1$  and at  $j = \ell$ . Therefore, using Eqs.(B1,B2), one obtains

$$\begin{bmatrix} (E + \mu) & \tau e^{-\frac{i}{2}\Phi} \\ \tau e^{\frac{i}{2}\Phi} & (E + \mu) \end{bmatrix} \begin{bmatrix} \bar{u}_1 \\ \bar{u}_\ell \end{bmatrix} = -w \begin{bmatrix} (u_2 - v_2) \\ (u_{\ell-1} + v_{\ell-1}) \end{bmatrix} \quad , \quad (\text{B3})$$

and

$$\begin{bmatrix} (E - \mu) & -\tau e^{\frac{i}{2}\Phi} \\ -\tau e^{-\frac{i}{2}\Phi} & (E - \mu) \end{bmatrix} \begin{bmatrix} \bar{v}_1 \\ \bar{v}_\ell \end{bmatrix} = -w \begin{bmatrix} (u_2 - v_2) \\ -(u_{\ell-1} + v_{\ell-1}) \end{bmatrix} \quad . \quad (\text{B4})$$

On inverting Eqs.(B3), one obtains

$$\begin{bmatrix} \bar{u}_1 \\ \bar{u}_\ell \end{bmatrix} = - \left\{ \frac{w}{(E + \mu)^2 - \tau^2} \right\} \begin{bmatrix} \{(E + \mu)(u_2 - v_2) - \tau e^{-\frac{i}{2}\Phi}(u_{\ell-1} + v_{\ell-1})\} \\ \{-\tau e^{\frac{i}{2}\Phi}(u_2 - v_2) + (E + \mu)(u_{\ell-1} + v_{\ell-1})\} \end{bmatrix} \quad , \quad (\text{B5})$$

while, on inverting Eqs.(B4), one rather gets

$$\begin{bmatrix} \bar{v}_1 \\ \bar{v}_\ell \end{bmatrix} = - \left\{ \frac{w}{(E - \mu)^2 - \tau^2} \right\} \begin{bmatrix} \{(E - \mu)(u_2 - v_2) - \tau e^{\frac{i}{2}\Phi}(u_{\ell-1} + v_{\ell-1})\} \\ \{\tau e^{-\frac{i}{2}\Phi}(u_2 - v_2) - (E - \mu)(u_{\ell-1} + v_{\ell-1})\} \end{bmatrix} \quad . \quad (\text{B6})$$

Now, setting  $j = 2, \ell - 1$ , one obtains the BdG equations

$$\begin{aligned} Eu_2 &= -w\{u_3 + \bar{u}_1\} - \mu u_2 + w\{v_3 - \bar{v}_1\} \\ Ev_2 &= -w\{u_3 - \bar{u}_1\} + w\{v_3 + \bar{v}_1\} + \mu v_2 \quad , \end{aligned} \quad (\text{B7})$$

and

$$\begin{aligned} Eu_{\ell-1} &= -w\{u_{\ell-2} + \bar{u}_\ell\} - \mu u_{\ell-1} + w\{\bar{v}_\ell - v_{\ell-2}\} \\ Ev_{\ell-1} &= -w\{\bar{u}_\ell - u_{\ell-2}\} + w\{\bar{v}_\ell + v_{\ell-2}\} + \mu v_{\ell-1} \quad . \end{aligned} \quad (\text{B8})$$

From Eqs.(B7,B8) we see that, in order for the solution in Eq.(B17) to hold for  $1 < j < \ell$ , one must have

$$\begin{aligned} \bar{u}_1 + \bar{v}_1 &= u_1 + v_1 \\ \bar{u}_\ell - \bar{v}_\ell &= u_\ell - v_\ell \quad , \end{aligned} \quad (\text{B9})$$

where, now,  $u_1, v_1$  ( $u_\ell, v_\ell$ ) denote the wavefunction  $u_j, v_j$  evaluated at  $j = 1$  ( $j = \ell$ ). Making a combined use of the above equations, one eventually gets to the consistency conditions given by

$$\begin{aligned} \bar{u}_1 + \bar{v}_1 &= -w \left\{ \frac{E + \mu}{(E + \mu)^2 - \tau^2} + \frac{E - \mu}{(E - \mu)^2 - \tau^2} \right\} (u_2 - v_2) + \tau w \left\{ \frac{e^{-\frac{i}{2}\Phi}}{(E + \mu)^2 - \tau^2} + \frac{e^{\frac{i}{2}\Phi}}{(E - \mu)^2 - \tau^2} \right\} (u_{\ell-1} + v_{\ell-1}) \\ \bar{u}_\ell - \bar{v}_\ell &= -w \left\{ \frac{E + \mu}{(E + \mu)^2 - \tau^2} + \frac{E - \mu}{(E - \mu)^2 - \tau^2} \right\} (u_{\ell-1} + v_{\ell-1}) + \tau w \left\{ \frac{e^{\frac{i}{2}\Phi}}{(E + \mu)^2 - \tau^2} + \frac{e^{-\frac{i}{2}\Phi}}{(E - \mu)^2 - \tau^2} \right\} (u_2 - v_2) \end{aligned} \quad (\text{B10})$$

We now make the ansatz that a generic solution of energy  $E$  takes the form

$$\begin{bmatrix} u_j \\ v_j \end{bmatrix}_+ = c \begin{bmatrix} \cos\left(\frac{\Psi}{2}\right) \{ae^{ikj} + be^{-ikj}\} \\ -i \sin\left(\frac{\Psi}{2}\right) \{ae^{ikj} - be^{-ikj}\} \end{bmatrix}, \quad (\text{B11})$$

with  $c$  being an appropriate normalization constant. Moreover, to simplify the notation, we set

$$\begin{aligned} \mathcal{A}(E) &= w \left\{ \frac{E + \mu}{(E + \mu)^2 - \tau^2} + \frac{E - \mu}{(E - \mu)^2 - \tau^2} \right\} \\ \mathcal{B}(E; \Phi) &= \tau w \left\{ \frac{e^{-\frac{i}{2}\Phi}}{(E + \mu)^2 - \tau^2} + \frac{e^{\frac{i}{2}\Phi}}{(E - \mu)^2 - \tau^2} \right\}. \end{aligned} \quad (\text{B12})$$

Therefore, we obtain the system of algebraic equations for  $a$  and  $b$  given by

$$\begin{aligned} \{e^{ik-i\frac{\Psi}{2}} + \mathcal{A}(E)e^{2ik+i\frac{\Psi}{2}} - \mathcal{B}[E; \Phi]e^{ik(\ell-1)-i\frac{\Psi}{2}}\}a + \{e^{-ik+i\frac{\Psi}{2}} + \mathcal{A}(E)e^{-2ik-i\frac{\Psi}{2}} - \mathcal{B}[E; \Phi]e^{-ik(\ell-1)+i\frac{\Psi}{2}}\}b &= 0 \\ \{e^{ik\ell+i\frac{\Psi}{2}} + \mathcal{A}(E)e^{ik(\ell-1)-i\frac{\Psi}{2}} - \mathcal{B}^*[E; \Phi]e^{2ik+i\frac{\Psi}{2}}\}a + \{e^{-ik\ell-i\frac{\Psi}{2}} + \mathcal{A}(E)e^{-ik(\ell-1)+i\frac{\Psi}{2}} - \mathcal{B}^*[E; \Phi]e^{-2ik-i\frac{\Psi}{2}}\}b &= 0 \end{aligned} \quad (\text{B13})$$

On requiring Eqs.(B13) to provide nontrivial solutions for  $a$  and  $b$ , one readily obtains the secular equation for the allowed values of the energy  $|E| > \Delta_w$  in the form

$$\begin{aligned} -\sin[k(\ell-1) + \Psi] - (\mathcal{A}^2(E) - |\mathcal{B}[E; \Phi]|^2) \sin[k(\ell-3) - \Psi] \\ -2\mathcal{A}(E) \sin[k(\ell-2)] + 2\Re e \mathcal{B}[E; \Phi] \sin[k + \Psi] = 0. \end{aligned} \quad (\text{B14})$$

Next, we consider the equation for subgap PMF energies. These correspond to complex values of  $k$  satisfying

$$\cos\left(\frac{k}{2}\right) = \pm i \sqrt{\frac{\Delta_w^2 - E^2}{8w\mu}}. \quad (\text{B15})$$

To solve Eq.(B15), we now define the momentum for particle-like excitations as  $k_p = \pi - i\delta$  and for hole-like excitations as  $k_h = \pi + i\delta$ , with

$$\delta = 2 \sinh^{-1} \left\{ \sqrt{\frac{\Delta_w^2 - E^2}{8w\mu}} \right\}. \quad (\text{B16})$$

As a result, one finds that the positive-energy PMF wavefunction is given by

$$\begin{bmatrix} u_j \\ v_j \end{bmatrix} = c (-1)^j \begin{bmatrix} \cosh\left(\frac{\xi}{2}\right) \{\alpha e^{j\delta} + \beta e^{-j\delta}\} \\ \sinh\left(\frac{\xi}{2}\right) \{\alpha e^{j\delta} - \beta e^{-j\delta}\} \end{bmatrix}, \quad (\text{B17})$$

with  $\xi$  defined through the equations

$$\begin{aligned} \cosh(\xi) &= \frac{2w \cosh(\delta) - \mu}{E} \\ \sinh(\xi) &= \frac{2w \sinh(\delta)}{E}, \end{aligned} \quad (\text{B18})$$

and the coefficients  $\alpha$  and  $\beta$  determined by the appropriate boundary conditions for the allowed wavefunctions. We therefore trade Eqs.(B10) for the following system in the unknowns  $\alpha, \beta$ :

$$\begin{aligned} \{e^{\delta+\frac{\xi}{2}} - e^{2\delta-\frac{\xi}{2}}\mathcal{A}(E) - e^{(\ell-1)\delta+\frac{\xi}{2}}\mathcal{B}(E; \Phi)\}\alpha + \{e^{-\delta-\frac{\xi}{2}} - e^{-2\delta+\frac{\xi}{2}}\mathcal{A}(E) - e^{-(\ell-1)\delta-\frac{\xi}{2}}\mathcal{B}(E; \Phi)\}\beta &= 0 \\ \{e^{\ell\delta-\frac{\xi}{2}} - e^{(\ell-1)\delta+\frac{\xi}{2}}\mathcal{A}(E) - e^{2\delta-\frac{\xi}{2}}\mathcal{B}^*(E; \Phi)\}\alpha + \{e^{-\ell\delta+\frac{\xi}{2}} - e^{-(\ell-1)\delta-\frac{\xi}{2}}\mathcal{A}(E) - e^{-2\delta+\frac{\xi}{2}}\mathcal{B}^*(E; \Phi)\}\beta &= 0. \end{aligned} \quad (\text{B19})$$

The system in Eq.(B19) admits a nontrivial solution for  $\alpha$  and  $\beta$  only provided that the following secular equation for the energy eigenvalue  $E$  is satisfied

$$-\sinh[(\ell-1)\delta - \xi] + 2\mathcal{A}(E) \sinh[(\ell-2)\delta] + 2\Re e(\mathcal{B}(E; \Phi)) \sinh[\delta - \xi] - \{\mathcal{A}^2(E) - |\mathcal{B}(E; \Phi)|^2\} \sinh[(\ell-3)\delta + \xi] = 0. \quad (\text{B20})$$

Clearly, Eqs.(B19,B20) are consistent with the solution for  $\tau = 0$ . Indeed, as  $\tau = 0$  (open chain limit), one obtains that (apart for a constant)  $\alpha = e^{-\frac{\xi}{2}}$  and  $\beta = -e^{\frac{\xi}{2}}$ . Also, we obtain that  $\mathcal{B}(E; \Phi) = 0$  and, as a result, Eqs.(B19) take the form

$$\begin{aligned} \{e^{\delta+\frac{\xi}{2}} - e^{2\delta-\frac{\xi}{2}}\mathcal{A}(E)\}\alpha + \{e^{-\delta-\frac{\xi}{2}} - e^{-2\delta+\frac{\xi}{2}}\mathcal{A}(E)\}\beta &= 0 \\ \{e^{\ell\delta-\frac{\xi}{2}} - e^{(\ell-1)\delta+\frac{\xi}{2}}\mathcal{A}(E)\}\alpha + \{e^{-\ell\delta+\frac{\xi}{2}} - e^{-(\ell-1)\delta-\frac{\xi}{2}}\mathcal{A}(E)\}\beta &= 0 \quad . \end{aligned} \quad (\text{B21})$$

Using the explicit expression for  $\mathcal{A}(E)$ , Eqs.(B21) yield

$$\begin{aligned} \alpha e^{\delta+\frac{\xi}{2}} + \beta e^{-\delta-\frac{\xi}{2}} - \left[ \frac{w}{E+\mu} + \frac{w}{E-\mu} \right] \{\alpha e^{2\delta-\frac{\xi}{2}} + \beta e^{-2\delta+\frac{\xi}{2}}\} &= 0 \\ \alpha e^{\ell\delta-\frac{\xi}{2}} + \beta e^{-\ell\delta+\frac{\xi}{2}} - \left[ \frac{w}{E+\mu} + \frac{w}{E-\mu} \right] \{\alpha e^{(\ell-1)\delta+\frac{\xi}{2}} + \beta e^{-(\ell-1)\delta-\frac{\xi}{2}}\} &= 0 \quad , \end{aligned} \quad (\text{B22})$$

that is

$$\begin{aligned} u_1 + v_1 + \left[ \frac{w}{E+\mu} + \frac{w}{E-\mu} \right] \{u_2 - v_2\} &= 0 \\ v_\ell - v_\ell + \left[ \frac{w}{E+\mu} + \frac{w}{E-\mu} \right] \{u_{\ell-1} + v_{\ell-1}\} &= 0 \quad . \end{aligned} \quad (\text{B23})$$

We now see that Eqs.(B23) respectively imply  $u_0 + v_0 = 0$ , and  $u_{\ell+1} - v_{\ell+1} = 0$ , which are the appropriate equations for  $\tau = 0$ . Of course, in general Eq.(B14,B20) for the PMF energy appear to be quite formidable and one has to numerically solve them to recover the functional dependence of the energy  $E$  on  $\Phi$ , just as we do in the main text. Nevertheless, one may effectively use Eq.(B20) to recover under which conditions, and at which values of  $\Phi = \Phi_*$ , the PMFs energy levels may cross each other, which is a key point in the application of our technique. In order to recover this point, we consider the zero-energy limit of Eq.(B20), thus obtaining

$$\mathcal{B}^2[0; \Phi_*] - 2\mathcal{B}[0; \Phi_*]e^{-(\ell-2)\delta_0} + e^{-2(\ell-2)\delta_0} = 0 \quad , \quad (\text{B24})$$

where we have taken into account that  $\mathcal{B}[0; \Phi]$  is real. Eq.(B24) is then solved by setting

$$\frac{2w\tau}{\mu^2 - \tau^2} \cos\left(\frac{\Phi_*}{2}\right) = e^{-(\ell-2)\delta_0} \Rightarrow \cos\left(\frac{\Phi_*}{2}\right) = \frac{\mu^2 - \tau^2}{2w\tau} e^{-(\ell-2)\delta_0} \quad . \quad (\text{B25})$$

Eq.(B25) admits real solutions for  $\Phi_*$  only provided that  $\left| \frac{\mu^2 - \tau^2}{2w\tau} e^{-(\ell-2)\delta_0} \right| \leq 1$ , which is always obeyed for either a long enough chain, or a large enough  $\tau$  (or both). A detailed discussion about this point is provided in the main text. Here, we point out an important consequence of Eq.(B25), namely, even for a finite-size ring, it is still possible to recover two zero-energy MMs, provided  $\Phi$  is properly tuned. To see this, at a given  $\Phi$ , we define the mode operators corresponding to the PMFs,  $\Gamma_0[\Phi]$ ,  $\Gamma_0^\dagger[\Phi]$ , respectively given by

$$\begin{aligned} \Gamma_0[\Phi] &= \sum_{j=1}^{\ell} \{[u_j]^* c_j + [v_j]^* c_j^\dagger\} \\ \Gamma_0^\dagger[\Phi] &= \sum_{j=1}^{\ell} \{u_j c_j^\dagger + v_j c_j\} \quad , \end{aligned} \quad (\text{B26})$$

with  $u_j, v_j$  being the wavefunctions in Eq.(B17). By definition, we then obtain

$$\begin{aligned} [\Gamma_0[\Phi], H] &= \epsilon_0[\Phi]\Gamma_0[\Phi] \\ [\Gamma_0^\dagger[\Phi], H] &= -\epsilon_0[\Phi]\Gamma_0^\dagger[\Phi] \quad , \end{aligned} \quad (\text{B27})$$

with  $\epsilon_0[\Phi]$  being the solution of Eq.(B20) at a given  $\Phi$ . Thus, for  $\Phi = \Phi_*$ , one obtains

$$[\Gamma_{0,*}, H] = [\Gamma_{0,*}^\dagger, H] = 0 \quad (\text{B28})$$

with  $\Gamma_{0,*} = \Gamma_0[\Phi = \Phi_*]$ . As a result, for  $\Phi = \Phi_*$  one may define the zero-mode MMs  $\gamma_1, \gamma_2$  by simply setting

$$\begin{aligned}\gamma_1 &= \Gamma_{0,*} + \Gamma_{0,*}^\dagger \\ \gamma_2 &= -i\{\Gamma_{0,*} - \Gamma_{0,*}^\dagger\} \quad .\end{aligned}\tag{B29}$$

As we discuss in the paper, the existence of  $\gamma_1, \gamma_2$  as zero-energy MMs is quite robust against the effects of disorder. For comparison, in the main text of the paper we also consider the dependence on  $\Phi$  of the subgap states in a superconducting ring made with an s-wave one-dimensional superconductor closed with a weak link of strength  $\tau$ . This is derived from the corresponding solution of the Bogoliubov-de Gennes equations for the wavefunction of a spin- $\sigma$  quasiparticle,  $u_j, v_j$  which, for the s-wave ring of length  $\ell$  and for the superconducting gap  $\Delta = w$  (in analogy to the simplifying limit we take above for the p-wave superconductor), are given by<sup>58</sup>

$$\begin{aligned}Eu_j &= -w\{u_{j+1} + u_{j-1}\} - \mu u_j + \sigma w v_j \\ Ev_j &= \sigma w v_j + w\{v_{j+1} + v_{j-1}\} + \mu v_j \quad ,\end{aligned}\tag{B30}$$

for  $1 < j < \ell$ , and by

$$\begin{aligned}Eu_1 &= -wu_2 - \tau e^{-\frac{i}{2}\Phi} u_\ell - \mu u_1 + \sigma w v_1 \\ Ev_1 &= \sigma w u_1 + w v_2 + \tau e^{\frac{i}{2}\Phi} v_\ell + \mu v_1 \quad ,\end{aligned}\tag{B31}$$

for  $j = 1$  and, finally, by

$$\begin{aligned}Eu_\ell &= -wu_{\ell-1} - \tau e^{\frac{i}{2}\Phi} u_1 - \mu u_\ell + \sigma w v_\ell \\ Ev_\ell &= \sigma w u_\ell + w v_{\ell-1} + \tau e^{-\frac{i}{2}\Phi} v_1 + \mu v_\ell \quad ,\end{aligned}\tag{B32}$$

for  $j = \ell$ . Eq.(B30) is solved by a wavefunction of the form

$$\begin{bmatrix} u_j \\ v_j \end{bmatrix} = \begin{bmatrix} u \\ v \end{bmatrix} e^{ikj} \quad ,\tag{B33}$$

provided  $u, v$  satisfy the secular equation

$$\begin{aligned}Eu &= -\{2w \cos(k) + \mu\}u + \sigma w v \\ Ev &= \sigma w u + \{2w \cos(k) + \mu\}v \quad .\end{aligned}\tag{B34}$$

Imposing the wavefunction in Eq.(B34) to satisfy Eqs.(B31,B32) as well implies the interface conditions across the weak link given by

$$\begin{aligned}0 &= wu_0 - \tau e^{-\frac{i}{2}\Phi} u_\ell \\ 0 &= wv_0 - \tau e^{\frac{i}{2}\Phi} v_\ell \\ 0 &= \tau e^{\frac{i}{2}\Phi} u_1 - wu_{\ell+1} \\ 0 &= \tau e^{-\frac{i}{2}\Phi} v_1 - wv_{\ell+1} \quad .\end{aligned}\tag{B35}$$

Let us, now, look for subgap solutions, with energy  $|E| < w$ . In this case, we obtain that  $k = \pm [\frac{\pi}{2} \pm iq]$ , and that, accordingly, the generic subgap solution is given by

$$\begin{bmatrix} u_j \\ v_j \end{bmatrix} = C \begin{bmatrix} (i^j e^{-qj} \alpha_{p,+} + i^{-j} e^{qj} \alpha_{p,-}) e^{\frac{i}{2}\xi} + (i^{-j} e^{-qj} \alpha_{h,+} + i^j e^{qj} \alpha_{h,-}) e^{-\frac{i}{2}\xi} \\ (i^j e^{-qj} \alpha_{p,+} + i^{-j} e^{qj} \alpha_{p,-}) e^{-\frac{i}{2}\xi} + (i^{-j} e^{-qj} \alpha_{h,+} + i^j e^{qj} \alpha_{h,-}) e^{\frac{i}{2}\xi} \end{bmatrix} \quad ,\tag{B36}$$

with

$$\begin{aligned}\sinh[q(E)] &= \sqrt{\frac{w^2 - E^2}{4w^2}} \\ \tan[\xi(E)] &= \sqrt{\frac{w^2 - E^2}{E^2}} \quad ,\end{aligned}\tag{B37}$$



and  $\alpha_{p,+}, \alpha_{p,-}, \alpha_{h,+}, \alpha_{h,-}$  coefficients. On requiring to recover a nontrivial solution for the above coefficients, one eventually finds the secular equation for the allowed energy eigenvalues, which is given by

$$4w\tau e^{\ell q}(e^{2q} - 1) \cos\left(\frac{\Phi}{2}\right) = 4w^2\{e^{2q(\ell+1)} - 1 + \tau^2(e^{2q} - e^{2q\ell})\} . \quad (\text{B38})$$

Eq.(B38) has been used to work out the subgap energy levels in the s-wave case, which have been discussed in the main text in comparison with the ones in the p-wave case.

- 
- <sup>1</sup> E. Majorana, *Il Nuovo Cimento* (1924-1942) **14**, 171 (2008).  
<sup>2</sup> A. Y. Kitaev, *Physics-Uspekhi* **44**, 131 (2001).  
<sup>3</sup> F. Wilczek, *Nature Physics* **5**, 614 (2009).  
<sup>4</sup> L. Fu and C. L. Kane, *Phys. Rev. Lett.* **100**, 096407 (2008).  
<sup>5</sup> L. Fu and C. L. Kane, *Phys. Rev. B* **79**, 161408 (2009).  
<sup>6</sup> C. Benjamin and J. K. Pachos, *Phys. Rev. B* **81**, 085101 (2010).  
<sup>7</sup> J. Nilsson, A. R. Akhmerov, and C. W. J. Beenakker, *Phys. Rev. Lett.* **101**, 120403 (2008).  
<sup>8</sup> R. M. Lutchyn, J. D. Sau, and S. Das Sarma, *Phys. Rev. Lett.* **105**, 077001 (2010).  
<sup>9</sup> Y. Oreg, G. Refael, and F. von Oppen, *Phys. Rev. Lett.* **105**, 177002 (2010).  
<sup>10</sup> J. Klinovaja, P. Stano, A. Yazdani, and D. Loss, *Phys. Rev. Lett.* **111**, 186805 (2013).  
<sup>11</sup> R. Pawlak, M. Kisiel, J. Klinovaja, T. Meier, S. Kawai, T. Glatzel, D. Loss, and E. Meyer, *npj Quantum Information* **2**, 16035 (2016).  
<sup>12</sup> M. Kjaergaard, K. Wölms, and K. Flensberg, *Phys. Rev. B* **85**, 020503 (2012).  
<sup>13</sup> T.-P. Choy, J. M. Edge, A. R. Akhmerov, and C. W. J. Beenakker, *Phys. Rev. B* **84**, 195442 (2011).  
<sup>14</sup> S. Nadj-Perge, I. K. Drozdov, B. A. Bernevig, and A. Yazdani, *Phys. Rev. B* **88**, 020407 (2013).  
<sup>15</sup> L. Fidkowski, J. Alicea, N. H. Lindner, R. M. Lutchyn, and M. P. A. Fisher, *Phys. Rev. B* **85**, 245121 (2012).  
<sup>16</sup> I. Affleck and D. Giuliano, *Journal of Statistical Mechanics: Theory and Experiment* **2013**, P06011 (2013).  
<sup>17</sup> I. Affleck and D. Giuliano, *Journal of Statistical Physics* **157**, 666 (2014).  
<sup>18</sup> B. Béri and N. R. Cooper, *Phys. Rev. Lett.* **109**, 156803 (2012).  
<sup>19</sup> B. Béri, *Phys. Rev. Lett.* **110**, 216803 (2013).  
<sup>20</sup> A. Altland, B. Béri, R. Egger, and A. M. Tsvelik, *Phys. Rev. Lett.* **113**, 076401 (2014).  
<sup>21</sup> E. Eriksson, A. Nava, C. Mora, and R. Egger, *Phys. Rev. B* **90**, 245417 (2014).  
<sup>22</sup> A. M. Tsvelik, *Phys. Rev. Lett.* **110**, 147202 (2013).  
<sup>23</sup> A. M. Tsvelik and W.-G. Yin, *Phys. Rev. B* **88**, 144401 (2013).  
<sup>24</sup> A. M. Tsvelik, *New Journal of Physics* **16**, 033003 (2014).  
<sup>25</sup> D. Giuliano, G. Campagnano, and A. Tagliacozzo, *The European Physical Journal B* **89**, 251 (2016).  
<sup>26</sup> N. Crampé and A. Trombettoni, *Nuclear Physics B* **871**, 526 (2013).  
<sup>27</sup> D. Giuliano, P. Sodano, A. Tagliacozzo, and A. Trombettoni, *Nuclear Physics B* **909**, 135 (2016).  
<sup>28</sup> D. Giuliano and P. Sodano, *EPL (Europhysics Letters)* **103**, 57006 (2013).  
<sup>29</sup> C. Nayak, S. H. Simon, A. Stern, M. Freedman, and S. Das Sarma, *Rev. Mod. Phys.* **80**, 1083 (2008).  
<sup>30</sup> D. A. Ivanov, *Phys. Rev. Lett.* **86**, 268 (2001).  
<sup>31</sup> V. Mourik, K. Zuo, S. M. Frolov, S. R. Plissard, E. P. A. M. Bakkers, and L. P. Kouwenhoven, *Science* **336**, 1003 (2012).  
<sup>32</sup> M. T. Deng, C. L. Yu, G. Y. Huang, M. Larsson, P. Caroff, and H. Q. Xu, *Nano Letters* **12**, 6414 (2012).  
<sup>33</sup> A. Das, Y. Ronen, Y. Most, Y. Oreg, M. Heiblum, and H. Shtrikman, *Nature Physics* **8**, 887 (2012).  
<sup>34</sup> E. J. H. Lee, X. Jiang, R. Aguado, G. Katsaros, C. M. Lieber, and S. De Franceschi, *Phys. Rev. Lett.* **109**, 186802 (2012).  
<sup>35</sup> H. O. H. Churchill, V. Fatemi, K. Grove-Rasmussen, M. T. Deng, P. Caroff, H. Q. Xu, and C. M. Marcus, *Phys. Rev. B* **87**, 241401 (2013).  
<sup>36</sup> P. Lucignano, F. Tafuri, and A. Tagliacozzo, *Phys. Rev. B* **88**, 184512 (2013).  
<sup>37</sup> G.-Q. Zha, L. Covaci, F. M. Peeters, and S.-P. Zhou, *Phys. Rev. B* **92**, 094516 (2015).  
<sup>38</sup> G.-Q. Zha and S.-P. Zhou, *EPL* **112**, 27009 (2015).  
<sup>39</sup> D. Giuliano and P. Sodano, *Nuclear Physics B* **711**, 480 (2005).  
<sup>40</sup> D. Giuliano and P. Sodano, *Nuclear Physics B* **770**, 332 (2007).  
<sup>41</sup> D. Giuliano and P. Sodano, *New Journal of Physics* **10**, 093023 (2008).  
<sup>42</sup> D. Giuliano and P. Sodano, *Nucl. Phys. B* **852**, 235 (2011).  
<sup>43</sup> D. Giuliano and P. Sodano, *EPL (Europhysics Letters)* **88**, 17012 (2009).  
<sup>44</sup> D. Giuliano and P. Sodano, *Nuclear Physics B* **837**, 153 (2010).  
<sup>45</sup> V. M. Fomin, *Physics of Quantum Rings* (Springer-Verlag, Berlin, 2014).  
<sup>46</sup> C. W. J. Beenakker, *Rev. Mod. Phys.* **69**, 731 (1997).  
<sup>47</sup> C. W. J. Beenakker, *Rev. Mod. Phys.* **87**, 1037 (2015).  
<sup>48</sup> A. Altland and M. R. Zirnbauer, *Phys. Rev. B* **55**, 1142 (1997).  
<sup>49</sup> O. Motrunich, K. Damle, and D. A. Huse, *Phys. Rev. B* **63**, 224204 (2001).

- <sup>50</sup> J. D. Sau and S. Das Sarma, Phys. Rev. B **88**, 064506 (2013).
- <sup>51</sup> P. W. Brouwer, M. Duckheim, A. Romito, and F. von Oppen, Phys. Rev. B **84**, 144526 (2011).
- <sup>52</sup> P. W. Brouwer, M. Duckheim, A. Romito, and F. von Oppen, Phys. Rev. Lett. **107**, 196804 (2011).
- <sup>53</sup> F. Pientka, G. Kells, A. Romito, P. W. Brouwer, and F. von Oppen, Phys. Rev. Lett. **109**, 227006 (2012).
- <sup>54</sup> F. Pientka, A. Romito, M. Duckheim, Y. Oreg, and F. von Oppen, New Journal of Physics **15**, 025001 (2013).
- <sup>55</sup> N. M. Gergs, L. Fritz, and D. Schuricht, Phys. Rev. B **93**, 075129 (2016).
- <sup>56</sup> W. DeGottardi, M. Thakurathi, S. Vishveshwara, and D. Sen, Phys. Rev. B **88**, 165111 (2013).
- <sup>57</sup> P. Jordan and E. Wigner, Z. Phys. **47**, 531 (1928).
- <sup>58</sup> A. Nava, R. Giuliano, G. Campagnano, and D. Giuliano, Phys. Rev. B **94**, 205125 (2016).
- <sup>59</sup> C. W. J. Beenakker, Three “Universal” Mesoscopic Josephson Effects (Springer Berlin-Heidelberg, Berlin, Heidelberg, 1992), pp. 235–253, ISBN 978-3-642-84818-6, URL [http://dx.doi.org/10.1007/978-3-642-84818-6\\_22](http://dx.doi.org/10.1007/978-3-642-84818-6_22).
- <sup>60</sup> A. R. Akhmerov, J. P. Dahlhaus, F. Hassler, M. Wimmer, and C. W. J. Beenakker, Phys. Rev. Lett. **106**, 057001 (2011).
- <sup>61</sup> J. Cayssol, T. Kontos, and G. Montambaux, Phys. Rev. B **67**, 184508 (2003).
- <sup>62</sup> K. T. Law, P. A. Lee, and T. K. Ng, Phys. Rev. Lett. **103**, 237001 (2009).
- <sup>63</sup> H.-J. Kwon, K. Sengupta, and V. M. Yakovenko, The European Physical Journal B - Condensed Matter and Complex Systems **37**, 349 (2004), ISSN 1434-6036.
- <sup>64</sup> L. Jiang, D. Pekker, J. Alicea, G. Refael, Y. Oreg, and F. von Oppen, Phys. Rev. Lett. **107**, 236401 (2011).
- <sup>65</sup> D. M. Badiane, M. Houzet, and J. S. Meyer, Phys. Rev. Lett. **107**, 177002 (2011).
- <sup>66</sup> L. P. Rokhinson, L. Xinyu, and J. K. Furdyna, Nature Physics **8**, 795 (2012).
- <sup>67</sup> J. D. Sau, S. Tewari, and S. Das Sarma, Phys. Rev. B **85**, 064512 (2012).
- <sup>68</sup> S. S. Hegde and S. Vishveshwara, Phys. Rev. B **94**, 115166 (2016).
- <sup>69</sup> M. Bocquet, D. Serban, and M. Zirnbauer, Nuclear Physics B **578**, 628 (2000), ISSN 0550-3213.
- <sup>70</sup> M. L. Mehta, Random Matrices (Elsevier Academic Press, Amsterdam, 2004).
- <sup>71</sup> D. Thouless, Physics Reports **13**, 93 (1974), ISSN 0370-1573.
- <sup>72</sup> J. T. Edwards and D. J. Thouless, Journal of Physics C: Solid State Physics **5**, 807 (1972).